DMD # 67504

Regulation of Hepatic Drug-metabolizing Enzymes in Germ-free mice by Conventionalization and Probiotics

Felcy Pavithra Selwyn, Sunny Lihua Cheng, Curtis D. Klaassen, and Julia Yue Cui

Affiliation:

Department of Environmental and Occupational Health Sciences

University of Washington

Seattle, WA 98105

Running Title:

Bacteria and Hepatic Drug-processing Genes

Send correspondence to:

Julia Yue Cui, PhD

Department of Environmental and Occupational Health Sciences
University of Washington
4225 Roosevelt Way NE, Seattle, WA, 98105
Email: juliacui@uw.edu
Tel: 206-616-4331

Word counts:

Text pages: 43
Tables: 1
Figures: 9
References: 37
Abstract: 248
Introduction: 749
Discussion: 1500

Abbreviations: Adh: alcohol dehydrogenase, Akr: aldo-keto reductase, Aldh: aldehyde dehydrogenase, *B. breve*: *Bifodobacterium breve*, *B. infantis*: *Bifidobacterium infantis*, *B. longum*: *Bifidobacterium longum,* Ces: carboxylesterase, ChIP: chromatin immunoprecipitation, Cyp: cytochrome P450, DME: drug-metabolizing enzyme, Ephx: epoxide hydrolase, Fmo: flavin containing monooxygenase, Gst: glutathione *S*-transferase, H3K4Me3: histone-3 lysine-4 tri-methylation, IGV: integrated genome viewer, *L. acidophilus*: *Lactobacillus acidophilus*, *L. bulgaricus*: *Lactobacillus bulgaricus*, *L. paracasei*: *Lactobacillus paracasei*, *L. plantarum*: *Lactobacillus plantarum*, Nqo1: NAD(P)H dehydrogenase quinone 1, Papss2: 3'-phosphoadenosine 5'-phosphosulfate synthase 2, Por: P450 oxidoreductase, PPARα: peroxisome proliferator activated receptor alpha, PXR: pregnane X receptor, RNA-Pol-II: RNA polymerase-II, *S. therm*: *Streptococcus thermophilus*, Sult: sulfotransferase, Ugt: UDP glucuronosyltransferase, TSS: transcription start site

DMD Fast Forward. Published on November 19, 2015 as DOI: 10.1124/dmd.115.067504
This article has not been copyedited and formatted. The final version may differ from this version.

ABSTRACT

Little is known regarding the effect of intestinal microbiota modifiers, such as probiotics and conventionalization with exogenous bacteria, on host hepatic drug metabolism. Therefore, the goal of this study was to determine the effect of these modifiers on the expression of various drug-metabolizing enzymes of the host liver. VSL3 is a probiotic that contains 8 live strains of bacteria. Five groups of mice were used: 1) conventional mice (CV), 2) conventional mice treated with VSL3 in drinking water, 3) germ-free (GF) mice, 4) GF mice treated with VSL3, and 5) GF mice exposed to the conventional environment for 2 months. All mice were 3-months-old at tissue collection. GF conditions markedly down-regulated the cytochrome P450 (Cyp) 3a gene cluster, but up-regulated the Cyp4a cluster, whereas conventionalization normalized their expression to conventional levels (RT-qPCR and western blot). Changes in the Cyp3a and 4a gene expression correlated with alterations in the PXR and PPARα-DNA binding, respectively (ChIP-qPCR). VSL3 increased each bacterial component in the large intestinal content of the CV mice, and increased these bacteria even more in GF mice, likely due to less competition for growth in the GF environment. VSL3 given to conventional mice increased the mRNAs of Cyp4v3, alcohol dehydrogenase 1, and carboxyesterase 2a, but decreased the mRNAs of multiple Phase-II glutathione-*S*-transferases. VSL3 given to germ-free mice decreased the mRNAs of UDP-glucuronosyl transferases 1a9 and 2a3. In conclusion, conventionalization and VSL3 alter the expression of many DMEs in liver, suggesting the importance of considering “bacteria-drug” interactions for various adverse drug reactions in patients.

INTRODUCTION

Intestinal microbiota modifiers, such as probiotics, antibiotics, and conventionalization to the environment, may both positively and negatively impact human health (Boyle et al., 2006; Carvalho et al., 2012; Kim, 2015; Vandenplas et al., 2015). Although the excessive use of antibiotics has raised concerns regarding their potential adverse health effects, leading to more stringent usage in medical practice, less is known regarding the safety of probiotics. Probiotics are defined as live microorganisms that confer a health benefit to the host when administered in adequate amounts (Sanders, 2008). VSL#3 (also called VSL3) is a combinatorial probiotic that is used for human intestinal disorders, such as inflammatory bowel disease and ulcerative colitis (Bibiloni et al., 2005; Penner and Fedorak, 2005; Mardini and Grigorian, 2014). VSL3 contains 8 live bacterial strains that are considered beneficial for the host, including *Bifidobacterium* (*B*.) *breve*, *B. longum*, *B. infantis*, *Lactobacillus* (*L*.) *acidophilus*, *L. plantarum*, *L. paracasei*, *L. bulgaricus*, and *Streptococcus* (*S*.) *thermophillus*. Even though there is evidence of beneficial effects and safety of VSL3 in animal models and clinical trials, little is known regarding the effect of VSL3 on the expression of various drug-metabolizing enzymes in liver, which is the major organ for drug detoxification. It is important to obtain this critical information, because altered expression of hepatic drug-metabolizing enzymes by VSL3 may lead to altered drug effects when VSL3 is co-administered with drugs.

Conventionalization, which is the exposure of the host to a microbial background in the environment, has attracted interest regarding its potential health benefits to humans. The “hygiene hypothesis” suggests that newborns delivered by cesarean section and raised in an overly clean environment may lack sufficient stimulation of the immune system, and

may be prone to develop chronic inflammatory conditions and obesity (Collado et al., 2015). In mice, colonization of germ-free (GF) mice during the neonatal period is helpful to establish immune signaling, whereas colonization of GF mice at 5-weeks of age leads to specific changes in chemokine signaling (Yamamoto et al., 2012). Conventionalization of the intestine of 8-week-old GF mice to a typical environmental microbial background impacts host intermediary metabolism, including increased body weight, stimulated hepatic glycogenesis and triglyceride synthesis, as well as altered bile acid composition (Claus et al., 2011). However, relatively less is known regarding the effect of colonization on xenobiotic metabolism in the liver of the host.

A major class of the Phase-I hepatic drug-metabolizing enzymes is the cytochrome P450s (Cyps), of which the Cyp1-3 family members are considered to be mainly responsible for xenobiotic metabolism, whereas the Cyp4 family members are responsible for lipid metabolism (Hardwick, 2008). It is well known that the aryl hydrocarbon receptor (AhR) transcriptionally up-regulates Cyp1 gene expression, the constitutive androstane receptor (CAR) up-regulates Cyp2b gene expression, and the pregnane X receptor (PXR) up-regulates Cyp3a gene expression in liver. Therefore, AhR, CAR, and PXR are often referred to as “xenobiotic-sensing transcription factors” (Xu et al., 2005). The peroxisome proliferator-activated receptor alpha (PPARα) is a lipid-sensor that up-regulates Cyp4a gene expression (Kroetz et al., 1998). Other important Phase-I enzymes involved in xenobiotic bioactivation and detoxification include alcohol dehydrogases (Adhs), aldehyde dehydrogenases (Aldhs), carboxyesterases (Cess), flavin containing monooxygenases (Fmos), aldo-keto reductases (Akrs), epoxide hydrolases (Ephx’s), and NAD(P)H dehydrogenase quinone

1 (Nqo1). Phase-II metabolism or conjugation reactions consist of the glutathione *S*-transferases (Gsts), UDP glucuronosyltransferases (Ugts), and sulfotransferases (Sults) that usually function as detoxification enzymes in the liver (Jancova et al., 2010). The xenobiotic- and lipid-sensing transcription factors noted above also regulate the expression of other non-Cyp Phase-I enzymes as well as Phase-II enzymes in liver (Alnouti and Klaassen, 2008; Knight et al., 2008; Buckley and Klaassen, 2009; Pratt-Hyatt et al., 2013). The GF mouse is an important model that allows mechanistic investigations on the role of intestinal microbiota on host drug metabolism. We have reported that certain Cyp3a genes are down-regulated, whereas certain Cyp4a genes are up-regulated in livers of GF mice (Selwyn et al., 2015a; Selwyn et al., 2015b).

The goal of this study was to systematically characterize the gene expression profiles of 94 drug-metabolizing enzymes (including Cyp3a and Cyp4a) in livers of 5 groups of mice: 1) conventional mice (CV), 2) CV treated with VSL3 in drinking water, 3) GF mice, 4) GF mice treated with VSL3, and 5) GF mice exposed to the conventional environment (GF+CV) for 2 months. We hypothesize that introducing exogenous bacteria, such as probiotics or conventionalization with bacteria from the environment, would partially restore mucosal mRNA expression of Cyp3a and 4a genes as well as other important drug-metabolizing enzymes.

MATERIALS AND METHODS

Animals and Procedures.

Male C57BL/6J CV mice were purchased from Jackson Laboratories (Bar Harbor, Maine). The initial breeding colony of GF C57BL/6J/UNC mice was established with

DMD Fast Forward. Published on November 19, 2015 as DOI: 10.1124/dmd.115.067504
This article has not been copyedited and formatted. The final version may differ from this version.

mice purchased from the National Gnotobiotic Rodent Resource Center (University of North Carolina, Chapel Hill). All mice used in the present study were housed in an AAALAC (Association for Assessment and Accreditation of Laboratory Animal Care International)-accredited facility at the University of Kansas Medical Center, with a 14-h light/10-h dark-cycle, in a temperature and humidity-controlled environment, and all mice had ad libitum access to autoclaved rodent chow and water. Starting at 2 months of age, CV and GF mice (male, n=6-8/group) were given the VSL3 probiotics in drinking water for 28 days, which includes a total of 4.5×10^6 CFU/ml of the following strains: *Lactobacillus (L.) acidophilus*, *L. bulgaricus*, *L. paracasei*, *L. plantarum*, *Bifidobacterium (B.) breve*, *B. infantis*, *B. longum*, and *Streptococcus (S.) thermophiles* (Sigma-Tau Pharmaceuticals, Inc. Gaithersburg, MD). In a separate study, 1-month old GF mice (male, n=4/group) were taken out of the germ-free isolator, and were housed in the same environment as the CV mice for two months.

All mice were euthanized with an overdose of pentobarbital at approximately 3-months of age. Livers were immediately frozen in liquid nitrogen. Small and large intestinal contents were flushed using phosphate buffered saline containing 10 mM dithiothreitol (DTT), and centrifuged at 20,000g for 30 min at 4°C as described previously (Zhang et al., 2012). All samples were stored in a -80°C freezer until further analyses. All animal procedures were approved by the Institutional Animal Care and Use Committee at the University of Kansas Medical Center.

Bacterial DNA Extraction and Quantification.

Total genomic bacterial DNA was extracted from the small and large intestinal contents of CV- and GF-mice (treated with or without VSL3), as well as conventionalized-GF (GF+CV) mice using the QIAmp DNA Stool Kit (Qiagen, Valencia, CA) according to the manufacturer's instructions. The concentration of total DNA was determined using a Qubit 2.0 Fluorometer (Life Technologies, Grand Island, NY). The 16S rRNA primers for the detection of *B. infantis* and *S. thermophilus* were described previously (Vitali et al., 2003; Furet et al., 2004). The 16S rRNA primers for the detection of *L. acidophilus*, *L. bulgaricus*, *L. plantarum*, *L. paracasei*, *B. breve*, and *B. longum* were designed based on the 16S rRNA bacterial amplicon sequences of these bacteria, and specificity was determined using NCBI BLAST against the 16S ribosomal RNA sequences (bacteria and archaea) database as shown in supplemental Table 1. The sequences for a pair of primers that recognize the universal bacterial 16S rRNA sequences was provided by the University of North Carolina Gnotobiotic core facilities. All primers were synthesized by Integrated DNA Technologies (Coralville, IA). The abundance of the genomic DNA encoding the bacterial 16S rRNAs in the intestinal content of mice was determined by quantitative polymerase chain reaction (qPCR) using a Bio-Rad CFX384 Real-Time PCR Detection System (Hercules, CA). Results are expressed as mean delta-delta cycle value (calculated as 2^[-(Cq - average reference Cq)] of the quantitative PCR (ddCq) as compared to the universal bacteria, per ng of DNA from the intestinal content. To validate the primers that target the VSL3 bacterial components of VSL3, the bacterial DNA from the pure VSL3 powder was extracted using the E.Z.N.A. Stool DNA Kit (Omega Bio-Tek Inc., Norcross, GA), and qPCR assays were performed using 1 ng, 3

ng, 10 ng, and 30 ng of total VSL3 DNA. Results are expressed as ddCq compared to the average Cq of the universal bacteria.

RNA isolation and mRNA Quantification of DPGs.

Total RNA was isolated from livers using RNA-Bee reagent (Tel-test Inc., Friendswood, TX) per the manufacturer's instructions. The concentration of total RNA was determined at 260nm using a NanoDrop 1000 Spectrophotometer (Thermo Scientific, Wilmington, DE). Reverse transcription was performed using an iScript cDNA Synthesis Kit (Bio-Rad, Hercules, CA). The resulting cDNA products were amplified by qPCR, using Sso Advanced Universal SYBR Green Supermix in a Bio-Rad CFX384 Real-Time PCR Detection System (Bio-Rad, Hercules, CA). The primers for all qPCR reactions were synthesized by Integrated DNA Technologies (Coralville, IA), and the primer sequences are shown in Supplemental Table 2. The results are expressed as % of the expression of the 18S rRNA.

Western blotting.

Hepatic microsomes were isolated from CV, GF, and conventionalized-GF (GF+CV) control mice, as well as VSL3-treated CV and GF mice, and protein concentrations were determined using the Qubit Protein Assay Kit (Life Technologies, Grand Island, NY) according to the manufacturer's instructions. The samples (50 µg of protein) were subjected to polyacrylamide gel electrophoresis and transferred onto a polyvinylidene difluoride (PVDF) membrane. Primary antibody against mouse Cyp3a11 (anti-rat CYP3A1/2 mAb, clone 2-13-1, 1:500) was a generous gift from Dr. Frank Gonzalez at the National Cancer Institute. Primary antibody against Cyp4a14 (goat polyclonal IgG,

1:500) was purchased from Santa Cruz Biotechnologies (Dallas, TX) (SC-46087). Primary antibody against mouse β-actin was purchased from Abcam (Cambridge, MA) (ab8227, 1:500). HRP-linked secondary antibodies were purchased from Sigma Aldrich (St. Louis, MO) and used at 1:2000 (namely rabbit anti-mouse A9044 for Cyp3a11, rabbit anti-goat A5420 for Cyp4a14, and goat anti-rabbit A6154 for β-actin). Proteins were detected using chemiluminescence (Thermo Fisher Scientific, Life Technologies, Grand Island, NY). Intensities of the protein bands were quantified using Image J Software (National Institutes of Health, Bethesda, MD).

Enzyme activities of Cyp3a and Cyp4a. Livers of mice were homogenized using a 2-mL glass homogenizer (Wheaton Co.) in ice-cold ST buffer of 250 mM sucrose in 10 mM Tris-HCl (pH 7.5). The homogenate was centrifuged (100,000g, 60 min) at 4 °C. The crude membrane pellet was re-suspended in ST buffer and stored at −80 °C. CYP enzyme activity determination was carried out following instructions from Promega. Twenty µg of protein was diluted to 12.5 µL and added to each well of a 96-well plate. 12.5 µL of the 4×CYP reaction mixture (12 µM Luciferin-IPA for CYP3A; 320 µM Luciferin-4A for CYP4A) was then added into each well and mixed gently. The plate was incubated at room temperature for 10 min. 25 µL of the 2× NADPH regeneration system was added into the CYP assays, mixed and incubated at the same temperature for 20 min. 50 µL of the reconstituted Luciferin detection reagent was added to the CYP assays and incubated at room temperature for another 20 min to stabilize the luminescent signal. Luminescence was recorded using a luminometer (PlateLumino system, MIDSCI Co., Valley Park, MO).

Chromatin immunoprecipitation (ChIP).

ChIP was performed using approximately 200 mg of frozen livers from CV-, GF-, and conventionalized-GF (GF+CV) mice, using the MAGnify Chromatin Immunoprecipitation System (Life Technologies, Grand Island, NY), with modifications. Briefly, livers were finely minced into less than 1 mm cubes using razor blades in cold 1×Dulbecco's Phosphate-Buffered Saline (D-PBS) in a sterile 10 cm culture dish on ice, and transferred into an ice-cold Dounce homogenizer (VWR International, Radnor, PA) to further grind the liver into a homogenous solution with a glass pestle. Samples were subjected to cross-linking using freshly prepared formaldehyde (final concentration: 1%), and rotated for 20 min at room temperature using an ELMI Intelli Mixer (ELMI Company, Riga, Latvia). The cross-linking was reversed by glycine (final concentration: 0.125 M) with rotation for 5 min at room temperature, followed by centrifugation to collect the pellets. The pellets were washed with cold D-PBS, and re-suspended using cold ChIP lysis buffer with a protease inhibitor cocktail (Sigma Alderich, St. Louis, MO), rotated at 4°C for 15 min, and centrifuged to obtain the pellets. The pellets were re-suspended in ChIP nuclear lysis buffer with protease inhibitors, and incubated on ice for 15 min. Chromatins were then fragmented into 300-500 bp average size-range using a Bioruptor UCD200 connected to a water-cooling system (Diagenode, Denville, NJ). The sonication condition was 10 × (30 sec on + 30 sec off) at 4°C, and was repeated after 10 min, at the highest intensity. The fragment size was confirmed by electrophoresis. ChIP-grade antibodies, namely SC-25381 (Santa Cruz, Dallas, TX) for PXR, NB600-636 (Novus Biologicals, Littleton, CO) for PPARα, and MMS-126R for RNA polymerase II (Covance, Emeryville, CA) were used for immunoprecipitation. An IgG antibody (ab18413, Abcam, Cambridge, MA) was used as a negative control. The immunoprecipitation procedures

are described in detail per the manufacturer's protocol (MAGnify Chromatin Immunoprecipitation System, Life Technologies, Grand Island, NY).

ChIP-qPCR primer design and qPCR reactions.

PXR- and PPARα-genomic DNA binding sites were obtained by re-analyzing the ChIP-Seq data in control C57BL/6 male mouse livers from previous publications (Cui et al., 2009; Lee et al., 2014). Nuclear receptor enrichment peaks were visualized by Integrated Genome Viewer (IGV) (Robinson et al., 2011), and the known DNA-binding motifs of PXR and PPARα, namely direct-repeat-3 (DR-3), DR-4, everted-repeat-6 (ER-6), and ER-8 for PXR, as well as DR-1 and DR-2 for PPARα (Cui et al., 2010; Lee et al., 2014) were determined using NUBIScan V2.0 (http://www.nubiscan.unibas.ch/). The qPCR primers were designed around the targeted motifs using NCBI Primer Design Tool (http://www.ncbi.nlm.nih.gov/tools/primer-blast/), and their specificities were confirmed using UCSC BLAT (https://genome.ucsc.edu/cgi-bin/hgBlat?command=start). The promoter sequences of Cyp3a and Cyp4a clusters were retrieved using the Mammalian Promoter Database (MPromDb, http://mpromdb.wistar.upenn.edu/). The qPCR primers for RNA-Pol-II were designed using the queried promoter sequences. Real-time qPCR reactions of the ChIP DNA were performed using SsoAdvanced Universal SYBR Green Supermix in a Bio-Rad CFX384 Real-Time PCR Detection System (Bio-Rad, Hercules, CA). The qPCR primer sequences, targeted genomic regions, as well as putative motifs are listed in supplemental Table 3.

Statistical Analysis.

Data are presented as mean ± SEM. Differences among multiple groups were determined by analysis of variance (ANOVA) followed by Duncan's Post Hoc test ($p<0.05$).

RESULTS

Bacterial quantification in the large intestinal content of VSL3-treated CV and GF mice, as well as in conventionalized-GF (GF+CV) mice.

To confirm the colonization of VSL3 bacterial components in the large intestinal contents of CV and GF mice treated with VSL3, qPCR analysis of bacterial 16S rRNA was performed using DNA isolated from the large intestinal content as described in MATERIALS AND METHODS. The bacteria found in VSL3 were also quantified in large intestinal content DNA samples of the conventionalized-GF (GF+CV) (conventionalized with the regular environment) mice, to determine whether these bacteria are present in the conventional animal-housing environment. Primers that recognize the universal bacterial 16S rRNA sequences were used to quantify changes in the total amount of bacteria following VSL3-treatment of CV and GF mice, as well as after conventionalization of GF+CV mice. To validate the robustness of all the 16S rRNA qPCR primers for bacterial detection, the bacterial DNA from the pure VSL3 powder at various concentrations was subjected to qPCR assays as shown in Supplemental Figure 1. Addition of 1 ng to 10 ng of VSL3 bacterial DNA input resulted in an increase in total bacteria detected (average Cq: 12.24, 10.83, and 10.02), whereas a decrease in the signal was observed at the highest concentration (30 ng), which is likely due to inhibition by an overwhelming amount of DNA templates (average Cq=18.26). Similarly, the 8

individual bacteria in VSL3 were detectable with high robustness at low and middle concentrations, whereas the middle and highest concentrations of VSL3 DNA input results in inhibition (Supplemental Fig. 1). In summary, the robustness of these 16S rRNA qPCR primers was confirmed for the follow-up analyses.

As shown in Figure 1, VSL3-treatment results in a 41% increase in the total bacteria in the large intestinal content of CV mice (as assessed by quantifying the universal bacteria). As expected, only background signals were detected in vehicle-treated GF mice (0.08% of vehicle-treated CV signals). As a result of the VSL3-treatment, there was a 652-fold increase in the signal detected in the large intestinal content of the GF mice. Conventionalization of GF mice also lead to a marked increase in the signal detected in the GF+CV large intestinal content (564-fold) as compared to the GF mice, and this is a result of the bacterial colonization from the conventional housing environment. The conventionalization of GF mice restored approximately 50% of total bacteria in the large intestine compared to the CV mice.

The *Bifodobacterium* bacteria in VSL3 are *B. breve*, *B. infantis*, and *B. longum* and they were detected only at background levels in the large intestinal contents of CV, GF, and GF+CV mice. VSL3 given to CV mice in the drinking water for 2 months increased the colonization of each of the *Bifodobacterium* components in the large intestinal content. Among these bacteria, *B. infantis* appeared to colonize the most in CV mice. Interestingly, in GF mice, VSL3 resulted in an even greater increase in the *Bifodobacterium* genus. Interestingly, *B. longum*, which colonized only to a minor extent in the large intestine of CV mice, became the dominant colonizer in the large intestinal content of GF mice. Within the *Lactobacillus* genus, *L. acidophilus*, *L. bulgaricus*, *L.*

paracasei, and *L. plantarum* are VSL3 components, and these bacteria were also minimally present in the large intestinal content of CV, GF, and conventionalized-GF (GF+CV) mice. In the large intestinal content of CV mice, VSL3 increased each of the *Lactobacillus* components, namely 405-fold for *L. acidophilus*, a 9.7-fold for *L. bulgaricus*, 47-fold for *L. plantarum*, and to a lesser extent (4.4-fold) for *L. paracasei*. In the large intestinal content of GF mice, VSL3 resulted in an even greater increase in all these *Lactobacilli*. The VSL3 component *Streptococcus thermophiles* increased 209-fold in CV and 442-fold in GF large intestinal content, and it was not present in the large intestinal content of the conventionalized GF mice. In summary, VSL3 treatment resulted in increased colonization of each of the 8 VSL3 bacteria components in the large intestinal content of CV mice, and an even higher colonization of these bacteria in the GF mice, likely due to the lack of competition with the endogenous residential bacteria in the large intestine. Conventionalization increased the total bacteria in the large intestinal content of the conventionalized-GF (GF+CV) mice, but generally did not markedly increase the VSL3 bacteria components in these mice, likely because these VSL3 bacteria are not abundant in the conventional housing environment.

In summary, VSL3 increased all the bacteria in the probiotic mixture in the large intestinal content of CV mice, and increased these bacteria even more in GF mice, likely due to less competition for bacterial growth in a GF-environment.

Expression of the Cyp3a gene cluster in livers of CV and GF mice following VSL3 treatment or conventionalization.

The Cyp3a gene family is well known to be responsible for oxidation of many drugs and other xenobiotics (Wilkinson, 1996). Similar to the human CYP3A gene cluster, the majority of the Cyp3a genes in mice also form a cluster (on chromosome 5), and these genes are: Cyp3a57, 3a16, 3a41a and 3a41b, 3a44, 3a11, 3a25, and 3a59 (Figure 2). Due to high sequence homology, a common pair of qPCR primers was designed for Cyp3a41a and 3a41b, and a common pair of qPCR primers was designed for Cyp3a25 and 3a59. Interestingly, the expression of the Cyp3a genes is “region-specific”, in that the mRNAs of Cyp3a41a/b, 3a44, 3a11, and 3a25/59 genes, which are located in the right portion of the Cyp3a gene cluster, all displayed a similar pattern following VSL3 treatment or conventionalization, more specifically: 1) VSL3 moderately decreased the mRNAs of Cyp3a44 and Cyp3a11, and tended to decrease Cyp3a41a/b and 3a25/59 (although a statistical significance was not achieved); 2) GF conditions markedly decreased the mRNAs of all these Cyps, and VSL3 was not able to normalize their expression in livers of GF mice; 3) conventionalization of GF mice partially restored the mRNAs of all of these Cyps to CV levels. In GF mice that were conventionalized, Cyp3a41a/b and Cyp3a11 mRNAs were completely normalized to CV levels, whereas Cyp3a44 and 3a25/29 mRNAs in livers of conventionalized-GF (GF+CV) mice were higher than livers of GF mice, but were only partially normalized when compared to expression in CV mice. Interestingly, for Cyp3a57 and 3a16, which are located in the left of the Cyp3a cluster, Cyp3a57 mRNA was minimally expressed in livers of all groups (Cq>30, data not shown); whereas Cyp3a16, which is a perinatal-specific Cyp3a isoform, was lowly expressed in CV, CV+VSL3, GF, GF+VSL3, and was only increased in the GF mice that were conventionalized. In summary, the chromatin region in the

Cyp3a gene cluster that is co-down-regulated by GF conditions but co-up-regulated by conventionalization is located in the right portion of the cluster. The regional-specific expression of Cyp3a mRNAs in the Cyp3a cluster suggests that certain epigenetic factors and/or transcription factors may contribute to the responsiveness to GF or conventionalization conditions as well as the basal expression of the Cyp3a genes.

Expression of the Cyp4a/b/x gene cluster in livers of CV and GF mice following VSL3 treatment or conventionalization.

The Cyp4a gene family members encode important fatty acid and prostaglandin ω-hydroxylases, and are highly inducible by PPARα ligands such as the hypolipidemic drugs (Kroetz et al., 1998). Similar to the human CYP4A cluster, the mouse Cyp4a genes form a cluster that are located on chromosome 4, together with Cyp4x1 and Cyp4b1 (Figure 3). Interestingly, the 4 Cyp4a genes in the middle of this cluster, namely Cyp4a14, 4a10, 4a31, and 4a32, all displayed a similar expression pattern: 1) VSL3 tended to increase the mRNAs of these Cyps in CV mouse livers, although statistical significance was not achieved; 2) GF conditions markedly increased the mRNAs of these Cyps in level of both GF and GF-VSL3 mice; 3) VSL3 did not alter the mRNAs of these Cyps in GF mice; and 4) conventionalization markedly reduced the mRNAs of these Cyps to conventional levels. In fact, there appeared to be an even further decrease in Cyp4a14 mRNA in livers of conventionalized GF mice, although a statistical significance was not achieved. In contrast, the Cyp4a genes located on the left (Cyp4x1, 4a29, 4a12a/b, and 30b), as well as Cyp4b1 located on the right boundary of the Cyp4a cluster, did not display the co-regulatory pattern. Cyp4x1 and 4a29 mRNAs were minimally expressed (Cq>30, data not shown); whereas Cyp4a30b, and 4b1 mRNAs

were not readily altered in any of the treatment groups; Cyp4a12a/b mRNA was higher in livers of GF mice compared to CV mice, and was not altered by VSL3. In summary, similar to the Cyp3a gene cluster, the expression of the Cyp4a/b/x gene cluster was also regional-specific, in that there appeared to be an active transcription region in the middle of the cluster that was co-regulated by VSL3, GF, and conventionalization conditions, whereas genes at the left and right boundaries of the cluster were either not expressed, or did not display a similar expression pattern as the 4 Cyp4a genes in the middle of the cluster.

In summary, the mRNA expression patterns for the Cyp3a and Cyp4a gene clusters indicate that VSL3 had a much less effect on their gene expression (a moderate decrease in the mRNAs of a couple of Cyp3as); GF conditions markedly decreased some Cyp3a mRNAs, but increased some Cyp4a mRNAs in a region-specific manner on the chromosomes, suggesting the presence of co-regulatory transcriptional mechanisms; and conventionalization of GF mice at least partially normalizes the Cyp3a and 4a gene expression to CV levels.

Western blotting analysis of Cyp3a11 and 4a14 protein expression in livers of CV and GF mice following VSL3 treatment or conventionalization.

Because the mRNAs of Cyp3a and 4a genes were altered by the intestinal microbiome, the protein expression of the representative Cyps, namely Cyp3a11 and 4a14, was determined by western blotting analysis (Figure 4). VSL3 did not alter the protein expression of Cyp3a11 or 4a14 in either the CV or GF mice. As expected, livers from GF- and VSL3-treated GF mice had a marked decrease in Cyp3a11 protein, but a

marked increase in Cyp4a14 protein (Figure 4A). Conventionalization of GF mice restored the protein expression of Cyp3a11 to CV control levels, and decreased Cyp4a14 protein to CV control levels (Figure 4B). Cyp4a14 mRNA also tended to be lower in livers of conventionalized GF mice as compared to livers of CV mice, although a statistical significance was not achieved (Figure 3). In summary, protein expression of Cyp3a11 and 4a11 was consistent with the mRNA data of these genes in livers of CV and GF mice following VSL3 treatment and conventionalization.

The effects of conventionalization on Cyp3a11 activity and Cyp4a14 activity in GF mice are shown in Figure 5. The results demonstrate that Cyp3a11 activity was decreased markedly in GF mice and increased to conventional levels after exposure to the conventional environment. However, Cyp4a14 activity was up-regulated in GF mice but was normalized to conventional levels by exposure to the conventional environment. The results are consistent with mRNA and protein expression levels in GF mice under conventionalization.

Expression of the Cyp4f gene cluster in livers of CV and GF mice following VSL3 treatment or conventionalization.

The CYP4F family in human liver microsomes is known to catalyze the omega oxidation of 3-hydroxy fatty acid and the initial oxidative O-demethylation of pafuramidine, which is an experimental drug for the treatment of pneumocystic pneumonia (Wang et al, 2006; Dhar et al., 2008). Regarding the mouse orthologs, the Cyp4f gene family members that form a cluster on chromosome 17 include Cyp4f39, Cyp4f17, 4f17, 4f37, 4f40, 4f15, 4f14, 4f13, and 4f41-ps (supplemental Figure 2). Cyp4f38, 4f41-ps, and Cyp4f40 were

minimally expressed in livers of all mouse groups (average Cq>30). Cyp4f13, 4f15, 4f16, and 4f37 mRNAs were not readily altered by any treatment. Cyp4f17 mRNA was not altered by VSL3 in CV or GF mice; however, its mRNA was up-regulated in GF conditions (with or without VSL3 treatment), as well as in livers of conventionalized GF mice. Cyp4f14 mRNA tended to be increased by VSL3 in CV mouse livers (although a statistical significance was not achieved), and was up-regulated in GF mouse livers. In summary, genes within the Cyp4f cluster do not appear to be co-regulated; Cyp4f17 and 4f14 mRNAs were the only Cyp4f genes that were differentially regulated by at least one of the three bacterial modification treatments. Both Cyp4f14 and 4f17 were up-regulated in GF conditions, whereas Cyp4f17 was further up-regulated by conventionalization.

Expression of other Cyps in livers of CV and GF mice following VSL3 treatment or conventionalization.

As shown in Figure 6, the mRNA of Cyp1a2, which is a prototypical target gene of the aryl hydrocarbon receptor (AhR) in liver, was not readily altered by VSL3 or conventionalization, however, it was up-regulated in livers of GF mice as compared to CV mice. The mRNAs of Cyp2b10 and 3a13 were not altered in any group of mice (supplemental Figure 3). Note that the Cyp3a13 gene is not part of the Cyp3a gene cluster described in Figure 2. Cyp4f18 mRNA was markedly increased in livers of GF mice (both control and VSL3-treated groups) as well as in livers of conventionalized GF mice. VSL3 also tended to increase Cyp4f18 mRNA in CV livers, although a statistical significance was not achieved. Cyp4v3 mRNA was increased markedly in livers from the VSL3-treated CV mice, GF mice, VSL3-treated GF mice, as well as conventionalized GF mice. The mRNA of cytochrome P450 oxidoreductase (Por), which is required for the

electron transfer from NADPH to the Cyps in the endoplasmic reticulum, was not markedly different in any of the groups.

Expression of alcohol dehydrogenase 1 (Adh1) and aldehyde dehydrogenases (Aldhs) in livers of CV and GF mice following VSL3 treatment or conventionalization.

Adhs and Aldhs are critical phase-I enzymes in the liver that metabolize alcohols and aldehydes. Adhs convert alcohols into aldehydes, whereas Aldhs further metabolize aldehydes into acids. VSL3 markedly increased the mRNA of Adh1 in livers of CV mice (Figure 7). However, the expression of Aldh1a7, 4a1, and 7a1 mRNAs were similar in all groups (supplemental Figure 3). GF conditions resulted in an increase in the mRNAs of Aldh1a1 and Aldh3a2, but a decrease in the mRNA of Aldh1b1 (Figure 7). Conventionalization of GF mice reduced Aldh3a2 mRNA back to conventional levels, but did not return the mRNAs of Aldh1a1 or Aldh1b1 back to conventional levels.

Expression of carboxylesterases (Cess), flavin-containing monooxygenases (Fmos), aldo-keto reductases (Akrs), epoxide hydrolase 1 (Ephx1), and NAD(P)H dehydrogenase quinone 1 (Nqo1) in livers of CV and GF mice following VSL3 treatment or conventionalization.

Cess are a group of important phase-I enzymes that hydrolyze carboxylic esters to form alcohols and carboxylates. The mRNAs of Ces1e/1g, Ces2c, and Ces3a were not readily altered by VSL3, GF, or conventionalized conditions; however, Ces2a mRNA was up-regulated by VSL3 in livers of CV mice but not in GF mice, whereas conventionalization of GF mice also increased Ces2a mRNA (Figure 7 and supplemental

Figure 3). Fmos are monooxygenases that oxygenate drugs and other xenobiotics**.** Fmo1, 2, and 4 mRNAs were similar in livers of all 5 groups of mice (supplemental Figure 4), however, Fmo5 mRNA was down-regulated in livers of GF mice (Figure 7). Akrs, Ephx1, and Nqo1 are phase-I enzymes that are involved in oxidation/reduction reactions. In general, the mRNAs of these genes were not readily altered by VSL3, GF, or conventionalized conditions, except that Akr1d1 mRNA was lower in livers of conventionalized GF mice (supplemental Figure 4).

Expression of glutathione *S*-transferases (Gsts) in livers of CV and GF mice following VSL3 treatment or conventionalization.

Gsts are an important family of phase-II enzymes that detoxify electrophiles by conjugating them with GSH. The mRNAs of Gstm1, m2, m3, and o1 were all down-regulated by VSL3 in livers of CV mice (Figure 8); Gstm4 mRNA also tended to be decreased by VSL3 in livers of CV mice, although a statistically significant difference was not achieved (supplemental Figure 5). Other Gst isoforms were not readily altered by VSL3 in livers of either CV or GF mice, except that Gsta1, a3, and a4 mRNAs, which tended to be increased in livers of VSL3-treated CV mice (as compared to control CV mice), although a statistically significant difference was not achieved; and this tendency disappeared in livers of VSL3-treated GF mice (supplemental Figure 6). GF conditions resulted in decreased mRNAs of Gstpi, m1, m2, m3, and o1 (Figure 8). The mRNAs of Gstm4 and t2 also tended to be lower in livers of GF mice, although a statistically significant difference was not achieved (supplemental Figure 6). Conventionalization of GF mice restored the Gstpi mRNA, but did not normalize the mRNAs of Gstm1, m2, m3, or o1 (Figure 8). In summary, multiple Gstm isoforms as well as Gsto1 were

DMD Fast Forward. Published on November 19, 2015 as DOI: 10.1124/dmd.115.067504
This article has not been copyedited and formatted. The final version may differ from this version.

down-regulated by VSL3; these genes as well as Gstpi were also down-regulated by GF conditions.

Expression of UDP-glucuronosyltransferases (Ugts) in livers of CV and GF mice following VSL3 treatment or conventionalization.

Ugts are a group of phase-II enzymes that catalyze the glucuronidation of substrates. As shown in Figure 8 and supplemental Figure 6, in general, most of the 12 Ugt mRNAs examined were not altered by any of the treatments, and these genes include Ugt1a1, 1a5, 1a6, 1a7, 2b5, 2b34, 2b35, and 2b36. VSL3 had no effect on the Ugt mRNA expression in livers of CV mice; however, it decreased the mRNAs of Ugt1a9 and 2a3 in livers of GF mice. GF conditions up-regulated the mRNAs of Ugt1a9 and 2b1. Conventionalization of GF mice reduced Ugt1a9 mRNA back to CV levels, and tended to reduce Ugt2a3 and 2b1 mRNAs to CV levels (although a statistical significance was not achieved), but markedly increased the mRNA of Ugt2b36/37/38.

Expression of sulfotransferases (Sults) in livers of CV and GF mice following VSL3 treatment or conventionalization.

Sults are a group of phase-II enzymes that catalyze the transfer of sulfate group from the co-substrate 3'-physphoadenosine-5'-phosphosulfate (PAPS) to alcohols or amines. PAPS synthase 2 (Papss2) is involved in the synthesis of the co-substrate of the sulfation reactions. The mRNAs of Sult2b1, 2a1, and 3a1 were minimally expressed in male mouse livers (average Cq>30, data not shown). The mRNAs of Sult1b1, 1d1, and Papss2 were not altered by any of the treatments (Figure s6). VSL3 had minimal effects on the expression of Sults; however, GF conditions markedly decreased Sult5a1 mRNA

(Figure 8, s6). GF mice colonized with bacteria from the CV environment had lower expression of Sult1a1 compared to GF mice colonized with VSL3 bacteria, indicating that different bacteria components have different effects on Sult1a1 gene expression.

ChIP-qPCR of DNA-binding fold-enrichment of PXR and RNA Pol II to the Cyp3a gene loci, as well as DNA-binding fold-enrichment of PPARα and RNA PolI II to the Cyp4a gene loci.

To determine the mechanistic involvement of PXR and PPARα in modulating the transcriptional regulation of the *Cyp3a* and *Cyp4a* clusters, ChIP was performed in livers of CV, GF, and conventionalized GF mice (2 independent pull-downs per receptor). Because VSL3 had minimal effects on the Cyp3a and Cyp4a gene expression, ChIP of VSL3 samples was not performed.

The constitutive PXR-DNA binding sites to the *Cyp3a* cluster in mouse liver were selected based on our previous publication (Cui et al., 2010), and the constitutive PPARα-DNA binding sites to the *Cyp4a* cluster in mouse liver were selected based on NCBI GEO Database Query dataset GSE61817 (Lee et al., 2014) (supplemental Figure 7). The PXR- and PPARα-DNA binding sites that are proximal to the transcription start sites of target genes were analyzed for putative DNA-binding motifs (namely DR-3, DR-4, ER-6, and ER-8 for PXR; as well as DR-1 and DR-2 for PPARα), and qPCR primers were designed centering the key motifs as noted in supplemental Table 3.

As shown in Figure 9, among the 5 selected PXR-DNA binding sites, Site 2 (-1.6kb upstream of *Cyp3a11*) displayed the highest PXR-DNA binding in livers of CV mice (26-fold), and GF conditions markedly decreased the PXR-DNA binding, whereas

conventionalization moderately restored the PXR-DNA binding (1.66-fold). Site 5 (-8.9kb upstream of *Cyp3a59*) displayed the second highest PXR-DNA binding fold-enrichment in livers of CV mice (4.77-fold), and GF conditions reduced the PXR-DNA binding to 2.08-fold, whereas conventionalization increased the PXR-DNA binding (8.47-fold). Site 1 (-90bp upstream of *Cyp3a11*) as well as Site 3 and Site 4 (-144bp and -1.9kb upstream of *Cyp3a25,* respectively) had low PXR-DNA binding in livers of CV mice, and GF conditions further reduced PXR-DNA binding to background levels, whereas conventionalization increased PXR-DNA binding in these regions. To confirm the functional significance of PXR-DNA binding to the *Cyp3a* cluster on gene transcription, quantification of RNA-Pol-II to the promoters of *Cyp3a11*, *3a25*, and *3a59* were analyzed by ChIP (due to high sequence similarity, the primers targeting specific promoters of other *Cyp* genes were not designed). Consistent with the PXR-DNA binding data, there was a marked decrease in RNA-Pol-II binding to the *Cyp3a11* promoter (from 3200-fold in CV mice to 15-fold in GF conditions), whereas conventionalization restored RNA-Pol-II binding approximately 2100-fold (Figure 9). RNA-Pol-II binding to *Cyp3a59* promoter decreased from 2039-fold (CV) to 30-fold (GF), whereas conventionalization moderately increased RNA-Pol-II binding (86-fold). Constitutive RNA-Pol-II binding to the *Cyp3a25* promoter was low (4.06-fold), whereas GF conditions further decreased the fold-enrichment to 1.55-fold, whereas RNA-Pol-II binding to conventionalized conditions was approximately 2.09-fold.

In regard to the *Cyp4a* cluster, PPARα-binding to Site 6 (approximately 4kb upstream of *Cyp4a10*) increased from 1.67-fold (CV) to 49-fold (GF), whereas conventionalization reduced PPARα-binding to 3.21-fold (Figure 9). Similarly, PPARα-binding to Site 7

(approximately 1kb downstream of TSS and within the first intron of *Cyp4a10*) increased from 10.75-fold (CV) to 36-fold (GF), whereas conventionalization reduced the PPARα-binding to 2.59-fold. PPARα-binding to the other regions, namely Site 8 and Site 9 (approximately -8.1kb upstream, and 930bp downstream [within the first intron] of *Cyp4a31*, respectively), and Site 10 (approximately 4kb upstream of Cyp4a32), followed a similar pattern, which was low PPARα-binding in livers of CV mice, increased PPARα-binding in livers of GF mice, and reduced PPARα-binding in livers of conventionalized GF mice. The RNA-Pol-II binding to the promoters of *Cyp4a14* and *4a32* was consistent with the PPARα-binding profiles. Due to high sequence similarity in the promoter regions, RNA-Pol-II binding to *Cyp4a10* and *4a31* was not performed.

In conclusion, the present study has shown that VSL3 in the drinking water of CV and GF mice resulted in successful colonization of the VSL3 bacterial components in the large intestine, but in general, VSL3 has a relatively minor effect on hepatic drug-metabolizing enzyme expression in mice. Germ-free conditions resulted in the most prominent changes in hepatic drug-metabolizing enzyme expression, most notably a consistent down-regulation of many genes in the *Cyp3a* cluster, but a consistent up-regulation of many genes in the *Cyp4a* cluster. Conventionalization of GF mice at least partially restores the expression of these genes to CV levels. The GF and conventionalization mediated changes in Cyp3a and 4a genes are associated with altered PXR and PPARα-binding to the targeted DNA sequences within these genes.

DISCUSSION

One of the interesting observations of the present study is the co-regulation of the *Cyp3a* and *Cyp4a* genes in specific genomic regions of polycistronic clusters. It is possible that distinct genomic regions within polycistron clusters are “hot zones” for trans-activation mediated by nuclear receptors such as PXR and PPARα, and this may be due to distinct histone epigenetic mechanisms (Barrera and Ren, 2006; Wang et al., 2009) that allow a permissive chromatin environment for PXR and PPARα to transcribe certain regions of a gene cluster. Indeed, previous studies using ChIP-Seq have also identified regional-specific localization of PXR and PPARα to the *Cyp3a* and *Cyp4a* clusters in mouse liver, respectively (Cui et al., 2010 for PXR; and Lee et al., 2014 for PPARα) (supplemental Figure 2). The interaction between intestinal microbiota and the hepatic histone epigenetic marks, as well as the subsequent effects on nuclear receptor recruitment of target genes, should be addressed in future studies.

The altered PXR- and PPARα-signaling in livers of GF and conventionalized GF mice are likely due to altered levels of bacterial metabolites in GF and conventionalization conditions. For PXR, secondary bile acids such as lithocholic acid, as well as indole 3-propionic acid (IPA), are known endogenous PXR activators (Staudinger et al., 2001; Venkatesh et al., 2014). For PPARα, it has been shown that the circadian rhythm gene Clock trans-activate the expression of PPARα (Oishi et al., 2005), and the Clock:Bmal1 target genes (such as Per1, 2, and 3) are markedly increased in livers of GF mice (data not shown), suggesting that the germ-free conditions may up-regulate the PPARα-signaling by enhancing the Bmal1:Clock-signaling. Future studies include colonized bacteria in conventionalized GF mice, to determine which bacteria are likely

responsible for increasing the PXR-signaling but suppressing the PPARα-signaling in liver.

Previously, the *bona fide* PXR- and PPARα-target genes that encode drug-metabolizing enzymes in mice have been determined using pharmacological and genetic approaches (Aleksunes and Klaassen, 2012). Cyp3a11, as well as Gstm1-3 have been shown to be *bona fide* PXR-target genes (Aleksunes and Klaassen, 2012). We have observed a down-regulation of the these genes in GF livers correlating with decreased PXR binding, and confirmed the critical involvement of PXR in the hepatic regulation of these genes following modifications in the intestinal microbiota (Figure 2 and 10). Similarly, Cyp4a14, Aldh1a1, and Aldh3a2 are *bona fide* PPARα-targets in liver (Aleksunes and Klaassen, 2012), and we has demonstrated an up-regulation of all of these genes in livers of GF mice, and this increase in Cyp4a14 and Aldh3a2 is completely reversed by conventionalization (Figure 3 and 7). The basal expression of Aldh1b1 and Sult5a1 has been shown to be suppressed by PPARα, as noted by increased Aldh1b1 Sult5a1 mRNA in livers of PPARα-null mice (Aleksunes and Klaassen, 2012); and the present study has also demonstrated a decrease in Aldh1b1 and Sult5a1 mRNAs in livers of GF mice, which was reversed by conventionalization of the GF mice (Figure 7 and 8). Therefore the alteration of Sult5a1 mRNAs in GF and conventionalized conditions is likely mediated through PPARα. PPARα-ChIP data on the Cyp4a cluster further demonstrated the role of PPARα in the hepatic regulation of target genes following modifications in the intestinal microbiota. Interestingly, Gstm1, m3, and m4 are also common target genes of both PXR and PPARα, evidenced by PXR-dependent up-regulation following PCN-treatment, and PPARα-dependent up-regulation following

clofibrate-treatment (Aleksunes and Klaassen, 2012). In the present study, the down-regulation of Gstm1-3 mRNAs (and a tendency to decrease Gstm4 mRNA) by VSL3-treatment and GF conditions suggests that the PXR effect is dominant over PPARα in regulating the expression of these genes. Conversely, Ugt1a9 mRNA has been shown to be increased by both PXR and PPARα ligands (PCN and clofibrate, respectively) (Aleksunes and Klaassen, 2012), whereas in the present study, Ugt1a9 mRNA is increased in livers of GF mice but reduced to CV levels in livers of conventionalized GF mice. Thus Ugt1a9 mRNA regulation may involve more PPARα than PXR following changes in intestinal microbiota. Certain drug-metabolizing enzymes, such as Ugt2b1, is down-regulated by PPARα, evidenced by decreased gene expression following PPARα-ligand treatment, but increased gene expression in PPARα-null mice (Aleksunes and Klaassen, 2012), but its mRNA is actually increased in livers of GF mice, where PPARα-signaling appears to be enhanced (Figure 7 and 8). Ugt1a1, 1a5, 2b35, and 2b36 mRNAs have been shown to be increased by PXR and PPARα-ligands (PCN and clofibrate, respectively) (Aleksunes and Klaassen, 2012), but they are not changed in GF or conventionalized conditions (Figure 8). The inconsistency in these observations suggests that additional regulatory factors are present in the expression of these Ugts.

The present findings of a decrease in expression of the Cyp3a genes and increase in expression of Cyp4a genes in livers of GF mice are consistent with our previous studies (Selwyn et al., 2015a; Selwyn et al., 2015b). The present results are also consistent with our previous studies in GF mice regarding the regulation of many other drug-metabolizing enzymes, such as Cyp1a2, Aldh1b1, Aldh3a2, Gstpi, Gstm3, and

Sult5a1 (Selwyn et al., 2015a; Selwyn et al., 2015b). The present observation of normalized Cyp3a11 gene expression in livers of GF mice after conventionalization is also consistent with previous studies using conventionalization or secondary bile acid replacement approaches (Toda et al., 2009; Claus et al., 2011). The contribution of the present study is that in addition to the previous knowledge on the effect of GF conditions on drug-processing gene expression, results of this study has systematically addressed the effects of the probiotic VSL3 and conventionalization on the expression of major drug-metabolizing enzymes in liver, and determined the putative PXR- and PPARα-binding to the *Cyp3a* and *Cyp4a* at the cluster-level, which provides mechanistic explanations of the gene expression profiles following changes in intestinal microbiota. There are certain genes for which the mRNAs are moderately altered in livers of GF in a previous RNA-Seq (Selwyn et al., 2015b), but were not altered in livers of GF mice the present study (such as Ces2a, Akr1c19, Cyp2b10, Cyp3a16, etc.). This inconsistency is likely due to different techniques used (RNA-Seq vs. RT-qPCR), vehicle effects, and/or statistical methods. Only moderate changes were reported between some genes in CV and GF mice in the previous study, whereas the trend is still present in the present study with many genes, but are not statistically significant.

The starting ages of the mice on VSL3 or conventionalization are different (2-month-old for VSL3 treatment, vs. 1-month-old for conventionalization). It is possible that the difference in the starting age will influence the regulation of drug metabolizing genes. It has been shown that early age conventionalization has more impact on the immune response signaling than late age exposure to the conventional microbial environment (Yamamoto et al., 2012). Thus it is also possible that early age exposure to VSL3 may

have different effect on drug-metabolizing enzyme expression. Regarding the duration of the VSL3 treatment, it has been shown that VSL3 supplementation for just 3-days profoundly alters the ileal microbiota composition in conventional mice, and improves the disease scores of dextran sodium sulfate induced colitis (Mar et al., 2014). Therefore, the 2-months treatment of VSL3 should be sufficient to alter the intestinal microbiota composition. However, it is likely that the duration of VSL3 is not long enough to markedly alter the expression of drug-metabolizing enzymes, and chronic treatment with VSL3 may produce different results.

The PXR binding to site 2, as well as RNA-Pol-II binding to Cyp3a59 in livers of GF+CV mice did not completely restore the CV conditions. It is possible that a moderate increase in the PXR/RNA-Pol-II binding) is sufficient to trans-activate the target gene expression; it is also possible that additional regulatory factors, such as permissive chromatin epigenetic marks and other transcription factors, facilitate the complete restoration of the Cyp3a11 gene expression in livers of GF+CV mice. This will need to be tested using an unbiased detection method such as RNA-Seq in future studies.

One potential concern regarding conventionalization procedures is that the types of bacteria introduced to GF+CV mice may be facility specific. It is likely that the exogenous bacteria gained in the GF+CV mice do not necessarily recapitulate the exogenous bacteria configuration in CV mice in terms of both quantity and composition, evidenced by a further increase in Cyp4f18, Cyp4v3, and Ugt2b36/37/38 mRNAs in livers of GF+CV mice as compared to CV mice. Specific bacterial strains in the intestine of conventionalized GF mice that are responsible for the changes in the PXR/PPARα-signaling and the expression of drug-metabolizing enzymes of the host

liver is not known, but a previous study using conventionalized C3H mice showed that *Enterococcaceae*, *Enterobacteriaceae*, *Lactobacillaceae*, *Erysipelotrichaceae*, and *Peptostreptococcaceae* are the first bacterial families to settle in the intestine after exposure to the local environment, whereas *Coriobacteriaceae* appears to link the liver and the intestine in host energy metabolism pathways (Claus et al., 2011). Future studies using 16S rRNA and metatranscriptome sequencing approaches will be helpful determine the specific bacterial strains that modulate the changes in hepatic drug-metabolizing enzyme expression, and subsequently administering these bacterial strains to GF mice will validate its contribution.

ACKNOWLEDGEMENTS

The authors would like to acknowledge Dr. Jerry Cangelosi as well as his laboratory members Connie Tzou and Kris Weigel, as well as Dr. Scott Meschke in the DEOHS, University of Washington, for their discussion and advice on bacterial quantification, as well as previous members in Dr. Klaassen's laboratory for help in tissue collection.

AUTHORSHIP CONTRIBUTIONS

Participated in the experimental design: Klaassen, Selwyn, Cui;

Conducting the experiments: Selwyn, Cui, Cheng;

Writing the manuscript: Cui, Klaassen, Selwyn, Cheng.

REFERENCES

Aleksunes LM and Klaassen CD (2012) Coordinated regulation of hepatic phase I and II drug-metabolizing genes and transporters using AhR-, CAR-, PXR-, PPARalpha-, and Nrf2-null mice. *Drug Metab Dispos* **40:**1366-1379.

Alnouti Y and Klaassen CD (2008) Regulation of sulfotransferase enzymes by prototypical microsomal enzyme inducers in mice. *J Pharmacol Exp Ther* **324:**612-621.

Barrera LO and Ren B (2006) The transcriptional regulatory code of eukaryotic cells--insights from genome-wide analysis of chromatin organization and transcription factor binding. *Curr Opin Cell Biol* **18:**291-298.

Bibiloni R, Fedorak RN, Tannock GW, Madsen KL, Gionchetti P, Campieri M, De Simone C, and Sartor RB (2005) VSL#3 probiotic-mixture induces remission in patients with active ulcerative colitis. *Am J Gastroenterol* **100:**1539-1546.

Boyle RJ, Robins-Browne RM, and Tang ML (2006) Probiotic use in clinical practice: what are the risks? *Am J Clin Nutr* **83:**1256-1264; quiz 1446-1257.

Buckley DB and Klaassen CD (2009) Induction of mouse UDP-glucuronosyltransferase mRNA expression in liver and intestine by activators of aryl-hydrocarbon receptor, constitutive androstane receptor, pregnane X receptor, peroxisome proliferator-activated receptor alpha, and nuclear factor erythroid 2-related factor 2. *Drug Metab Dispos* **37:**847-856.

Carvalho BM, Guadagnini D, Tsukumo DM, Schenka AA, Latuf-Filho P, Vassallo J, Dias JC, Kubota LT, Carvalheira JB, and Saad MJ (2012) Modulation of gut microbiota by antibiotics improves insulin signalling in high-fat fed mice. *Diabetologia*

55:2823-2834.

Claus SP, Ellero SL, Berger B, Krause L, Bruttin A, Molina J, Paris A, Want EJ, de Waziers I, Cloarec O, Richards SE, Wang Y, Dumas ME, Ross A, Rezzi S, Kochhar S, Van Bladeren P, Lindon JC, Holmes E, and Nicholson JK (2011) Colonization-induced host-gut microbial metabolic interaction. *MBio* **2:**e00271-00210.

Collado MC, Rautava S, Isolauri E, and Salminen S (2015) Gut microbiota: a source of novel tools to reduce the risk of human disease? *Pediatr Res* **77:**182-188.

Cui JY, Gunewardena SS, Rockwell CE, and Klaassen CD (2010) ChIPing the cistrome of PXR in mouse liver. *Nucleic Acids Res* **38:**7943-7963.

Dhar M , Sepkovic DW, Hirani V, Magnusson RP, Lasker JM (2008) Omega oxidation of 3-hydroxy fatty acids by the human CYP4F gene subfamily enzyme CYP4F11. *J Lipid Res* **49:**612.

Furet JP, Quenee P, and Tailliez P (2004) Molecular quantification of lactic acid bacteria in fermented milk products using real-time quantitative PCR. *Int J Food Microbiol* **97:**197-207.

Hardwick JP (2008) Cytochrome P450 omega hydroxylase (CYP4) function in fatty acid metabolism and metabolic diseases. *Biochem Pharmacol* **75:**2263-2275.

Jancova P, Anzenbacher P, and Anzenbacherova E (2010) Phase II drug metabolizing enzymes. *Biomed Pap Med Fac Univ Palacky Olomouc Czech Repub* **154:**103-116.

Kim DH (2015) Gut Microbiota-Mediated Drug-Antibiotic Interactions. *Drug Metab Dispos*. 43: 1581-9.

Knight TR, Choudhuri S, and Klaassen CD (2008) Induction of hepatic glutathione S-transferases in male mice by prototypes of various classes of microsomal enzyme inducers. *Toxicol Sci* **106:**329-338.

Kroetz DL, Yook P, Costet P, Bianchi P, and Pineau T (1998) Peroxisome proliferator-activated receptor alpha controls the hepatic CYP4A induction adaptive response to starvation and diabetes. *J Biol Chem* **273:**31581-31589.

Lee JH, Moon G, Kwon HJ, Jung WJ, Seo PJ, Baec TY, and Kim HS (2012) [Effect of a probiotic preparation (VSL#3) in patients with mild to moderate ulcerative colitis]. *Korean J Gastroenterol* **60:**94-101.

Lee JM, Wagner M, Xiao R, Kim KH, Feng D, Lazar MA, and Moore DD (2014) Nutrient-sensing nuclear receptors coordinate autophagy. *Nature* **516:**112-115.

Mar JS, Nagalingam NA, Song Y, Onizawa M, Lee JW, Lynch SV (2014) Amelioration of DSS-induced murine colitis by VSL#3 supplementation is primarily associated with changes in ileal microbiota composition. *Gut Microbes* **4**: 494-503.

Mardini HE and Grigorian AY (2014) Probiotic mix VSL#3 is effective adjunctive therapy for mild to moderately active ulcerative colitis: a meta-analysis. *Inflamm Bowel Dis* **20:**1562-1567.

Oishi K, Shirai H, and Ishida N (2005) CLOCK is involved in the circadian transactivation of peroxisome-proliferator-activated receptor alpha (PPARalpha) in mice. *Biochem J* **386:**575-581.

Penner RM and Fedorak RN (2005) Probiotics in the management of inflammatory bowel disease. *MedGenMed* **7:**19.

Pratt-Hyatt M, Lickteig AJ, and Klaassen CD (2013) Tissue distribution, ontogeny, and chemical induction of aldo-keto reductases in mice. *Drug Metab Dispos*

41:1480-1487.

Sanders ME (2008) Probiotics: definition, sources, selection, and uses. *Clin Infect Dis* **46 Suppl 2:**S58-61; discussion S144-151.

Selwyn FP, Cheng SL, Bammler TK, Prasad B, Vrana M, Klaassen C, and Cui JY (2015a) Developmental regulation of drug-processing genes in livers of germ-free mice. *Toxicol Sci*. 147: 84-103.

Selwyn FP, Cui JY, and Klaassen CD (2015b) RNA-Seq quantification of hepatic drug processing genes in germ-free mice. *Drug Metab Dispos*. 43: 1572-80.

Staudinger JL, Goodwin B, Jones SA, Hawkins-Brown D, MacKenzie KI, LaTour A, Liu Y, Klaassen CD, Brown KK, Reinhard J, Willson TM, Koller BH, and Kliewer SA (2001) The nuclear receptor PXR is a lithocholic acid sensor that protects against liver toxicity. *Proc Natl Acad Sci U S A* **98:**3369-3374.

Toda T, Saito N, Ikarashi N, Ito K, Yamamoto M, Ishige A, Watanabe K, and Sugiyama K (2009) Intestinal flora induces the expression of Cyp3a in the mouse liver. *Xenobiotica* **39:**323-334.

Vandenplas Y, Huys G, and Daube G (2015) Probiotics: an update. *J Pediatr (Rio J)* **91:**6-21.

Venkatesh M, Mukherjee S, Wang H, Li H, Sun K, Benechet AP, Qiu Z, Maher L, Redinbo MR, Phillips RS, Fleet JC, Kortagere S, Mukherjee P, Fasano A, Le Ven J, Nicholson JK, Dumas ME, Khanna KM, and Mani S (2014) Symbiotic bacterial metabolites regulate gastrointestinal barrier function via the xenobiotic sensor PXR and Toll-like receptor 4. *Immunity* **41:**296-310.

Vitali B, Candela M, Matteuzzi D, and Brigidi P (2003) Quantitative detection of probiotic

Bifidobacterium strains in bacterial mixtures by using real-time PCR. *Syst Appl Microbiol* **26:**269-276.

Wang MZ, Saulter JY, Usuki E, Cheung YL, Hall M, Bridges AS, Loewen G, Parkinson OT, Stephens CE, Allen JL, Zeldin DC, Boykin DW, Tidwell RR, Parkinson A, Paine MF, and Hall JE (2006) CYP4F enzymes are the major enzymes in human liver microsomes that catalyze the O-demethylation of the antiparasitic prodrug DB289 [2,5-bis(4-amidinophenyl)furan-bis-O-methylamidoxime]. *Drug Metab Dispos* **34:**1985.

Wang Z, Schones DE, and Zhao K (2009) Characterization of human epigenomes. *Curr Opin Genet Dev* **19:**127-134.

Wilkinson GR (1996) Cytochrome P4503A (CYP3A) metabolism: prediction of in vivo activity in humans. *J Pharmacokinet Biopharm* **24:**475-490.

Xu C, Li CY, and Kong AN (2005) Induction of phase I, II and III drug metabolism/transport by xenobiotics. *Arch Pharm Res* **28:**249-268.

Yamamoto M, Yamaguchi R, Munakata K, Takashima K, Nishiyama M, Hioki K, Ohnishi Y, Nagasaki M, Imoto S, Miyano S, Ishige A, and Watanabe K (2012) A microarray analysis of gnotobiotic mice indicating that microbial exposure during the neonatal period plays an essential role in immune system development. *BMC Genomics* **13:**335.

FOOTNOTES

This work was supported by National Institutes of Health [GM111381] and [ES019487], as well as start-up funds from University of Washington Center of Ecogenetics and Environmental Health [P30 ES0007033].

FIGURE LEGENDS

Figure 1. The 16S rRNA abundance of universal bacteria, as well as the 8 bacterial components in VSL3, namely *B. breve, B. infantis, B. longum, L. acidophilus, L. bulgaricus, L. plantarum, L. paracasei*, and *S. thermophilus*, in the large intestinal content. DNA samples from CV, CV+VSL3, GF, GF+VSL3, and conventionalized-GF (GF+CV) groups. Large intestinal content DNA was extracted as described in MATERIALS AND METHODS, and 5.6 ng of total DNA was loaded in each well of the qPCR reactions. Results are expressed as delta-delta cycle value (calculated as 2^[-(Cq - average reference Cq)] of the quantitative PCR (ddCq) as compared to the universal bacteria.

Figure 2. The mRNA expression of the Cyp3a gene cluster (namely Cyp3a41a/b, 3a44, 3a11, 3a25/59, 3a57, and 3a16) in liver samples from CV, CV+VSL3, GF, GF+VSL3, and GF+CV groups. The genomic locations of the Cyp3a genes are displayed using the Integrated Genome Viewer (IGV). RT-qPCR for each gene was performed as described in MATERIALS AND METHODS. Data are expressed as % of the housekeeping gene 18S rRNA. Statistical analysis was performed using ANOVA followed by Duncan's Post Hoc Test with $p<0.05$ considered statistically significant. Treatment-groups that are not statistically different are labeled with the same letter.

Figure 3. The mRNA expression of the Cyp4a gene cluster (namely Cyp4a14, 4a10, 4a31, 4a32, 4x1, 4a29, 4a12a/b, 4a30b, and 4b1) in liver samples from CV, CV+VSL3, GF, GF+VSL3, and GF+CV groups. The genomic locations of the Cyp4 genes are displayed using the Integrated Genome Viewer (IGV). RT-qPCR for each gene was performed as described in MATERIALS AND METHODS. Data are expressed as % of

the housekeeping gene 18S rRNA. Statistical analysis was performed using ANOVA followed by the Duncan's Post Hoc Test with $p<0.05$ considered statistically significant. Treatment-groups that are not statistically different are labeled with the same letter.

Figure 4. A. Protein expression in livers of CV and GF mice treated with vehicle or VSL3 (n=3 per group). **B.** Protein expression by western blots in livers of control CV, GF, and GF+CV mice (n=3 per group). Western blotting of Cyp3a11, Cyp4a14, and β-actin proteins in hepatic microsomes were quantified as described in MATERIALS AND METHODS. Quantification of protein band intensities after normalization to the loading control β-actin was performed using Image J software. Statistical analysis was performed using ANOVA followed by the Duncan's PostHoc Test with $p<0.05$ considered statistically significant. Treatment-groups that are not statistically different are labeled with the same letter.

Figure 5. Enzyme activities of Cyp3a (A) and Cyp4a (B) in crude membranes of livers from CV, GF, and GF+CV mice. CYP enzyme activity determination was carried out according to the manufacturer's protocol as described in the Materials and Methods. Asterisks refer to statistically significant differences as compared to CV mice.

Figure 6. The mRNA expression of Cyp1a2, 4f18, 4v3, and Por in liver samples from CV, CV+VSL3, GF, GF+VSL3, and GF+CV groups. RT-qPCR for each gene was performed as described in MATERIALS AND METHODS. Data are expressed as % of the housekeeping gene 18S rRNA. Statistical analysis was performed using ANOVA followed by the Duncan's Post Hoc Test with $p<0.05$ considered statistically significant. Treatment-groups that are not statistically different are labeled with the same letter.

Figure 7. The mRNA expression of Adh1, Aldh1a1, Aldh1b1, Aldh3a2, Ces1e/1g, Ces2a, and Fmo5 in liver samples from CV, CV+VSL3, GF, GF+VSL3, and GF+CV groups. RT-qPCR for each gene was performed as described in MATERIALS AND METHODS. Data are expressed as % of the housekeeping gene 18S rRNA. Statistical analysis was performed using ANOVA followed by the Duncan's Post Hoc Test with $p<0.05$ considered statistically significant. Treatment-groups that are not statistically different are labeled with the same letter.

Figure 8. The mRNA expression of Gstpi, Gstm1-m3, Gsto1, Ugt1a9, Ugt2a3, Ugt2b1, Ugt2b36/37/38, and Sult5a1 in liver samples from CV, CV+VSL3, GF, GF+VSL3, and GF+CV groups. RT-qPCR for each gene was performed as described in MATERIALS AND METHODS. Data are expressed as % of the housekeeping gene 18S rRNA. Statistical analysis was performed using ANOVA followed by the Duncan's Post Hoc Test with $p<0.05$ considered statistically significant. Treatment-groups that are not statistically different are labeled with the same letter.

Figure 9. ChIP-qPCR of the DNA binding for PXR and RNA Pol II to the *Cyp3a* gene loci, as well as PPARα and RNA-Pol-II to the Cyp4a gene loci. For PXR, sites 1-5 were selected based on the re-analysis of a published PXR-ChIP-Seq experiment in control adult conventional male mouse livers (Cui et al., 2010), and qPCR primers were designed centering the known PXR-DNA binding motifs (DR-3, DR-4, ER-6, and ER-8) in these regions. For PPARα, sites 6-10 were selected based on the re-analysis of a published PPARα ChIP-Seq experiment in control adult conventional male mouse livers (NCBI GEO Database Query dataset GSE61817, Lee et al., 2014), and qPCR primers were designed centering the known PPARα-DNA binding motif DR-2 in these regions.

For RNA Pol II, qPCR primers were designed centering the TATA box within the promoters of the target genes. ChIP assays were performed using specific antibodies against PXR, PPARα, RNA Pol II, and IgG as described in MATERIALS AND METHODS. Data were first normalized to genomic DNA input, and then expressed as fold-enrichment over IgG control.

DMD Fast Forward. Published on November 19, 2015 as DOI: 10.1124/dmd.115.067504
This article has not been copyedited and formatted. The final version may differ from this version.

Table 1. Summary of DPGs that are differentially regulated in response to gut microbiota modifiers

Gut microbiota modifiers	Up-regulated drug-metabolizing enzymes	Down-regulated drug-metabolizing enzymes
VSL3 (as compared to control groups of the same mouse model)	**Phase-I:** Cyp4v3 (4.26-fold), Adh1 (2.23-fold), Ces2a (2.07-fold)	**Phase-I:** Cyp3a44 (67.42%), Cyp3a11 (59.88%)
	Phase-II: none observed	**Phase-II:** Gstm1 (65.50%), Gstm2 (49.86%), Gstm3 (61.58%), Gsto1 (63.62%), Ugt1a9* (54.41%), Ugt2a3* (52.24%)
Germ free (as compared to control CV mice)	**Phase-I:** Cyp4a cluster (Cyp4a14 [9.84-fold], 4a10 [53.34-fold], 4a31 [5.86-fold], 4a32 [6.06-fold], 4a12a/b [2.20-fold]), Cyp4f17 (1.86-fold), Cyp4f14 (5.30-fold), Cyp4f18 (19.83-fold), Cyp4v3 (2.88-fold), Cyp1a2 (1.64-fold), Aldh1a1 (2.03-fold); Aldh3a1 (3.08-fold), Aldh3a2 (2.03-fold)	**Phase-I:** Cyp3a cluster (Cyp3a41a/b [16.18%], 3a44 [11.33%], 3a11 [10.69%], 3a25/59 [32.44%]), Aldh1b1 (41.30%), Fmo5 (54.43%)
	Phase-II: Ugt1a9 (1.68-fold), Ugt2b1 (1.83-fold)	**Phase-II:** Gstpi (57.71%), Gstm1 (53.15%), Gstm2 (29.70%), Gstm3 (34.28%), Gsto1 (49.36%), Sult5a1 (36.39%)
Conventionalization (as compared to control GF mice)	**Phase-I:** Cyp3a cluster (Cyp3a41a/b [6.38-fold], 3a44 [1.60-fold], 3a11 [7.56-fold], 3a25/59, 3a16 [7.12-fold]), Cyp4f17 (1.47-fold), Ces2a (1.86-fold)	**Phase-I:** Cyp4a cluster (Cyp4a14 [0.98%], 4a10 [6.51%], 4a31 [11.42%], 4a32 [7.43%], 4a12a/b [59.22%]), Aldh3a2 [20.17%], Ces1e/1g [42.60%], Akr1d1 (39.02%)
	Phase-II: Gstpi (2.01-fold), Ugt2a36/37/38 (6.01-fold), Sult5a1 (2.88-fold)	**Phase-II:** Ugt1a9 (53.19%)

(*Differentially regulated in GF livers)

Figure 1

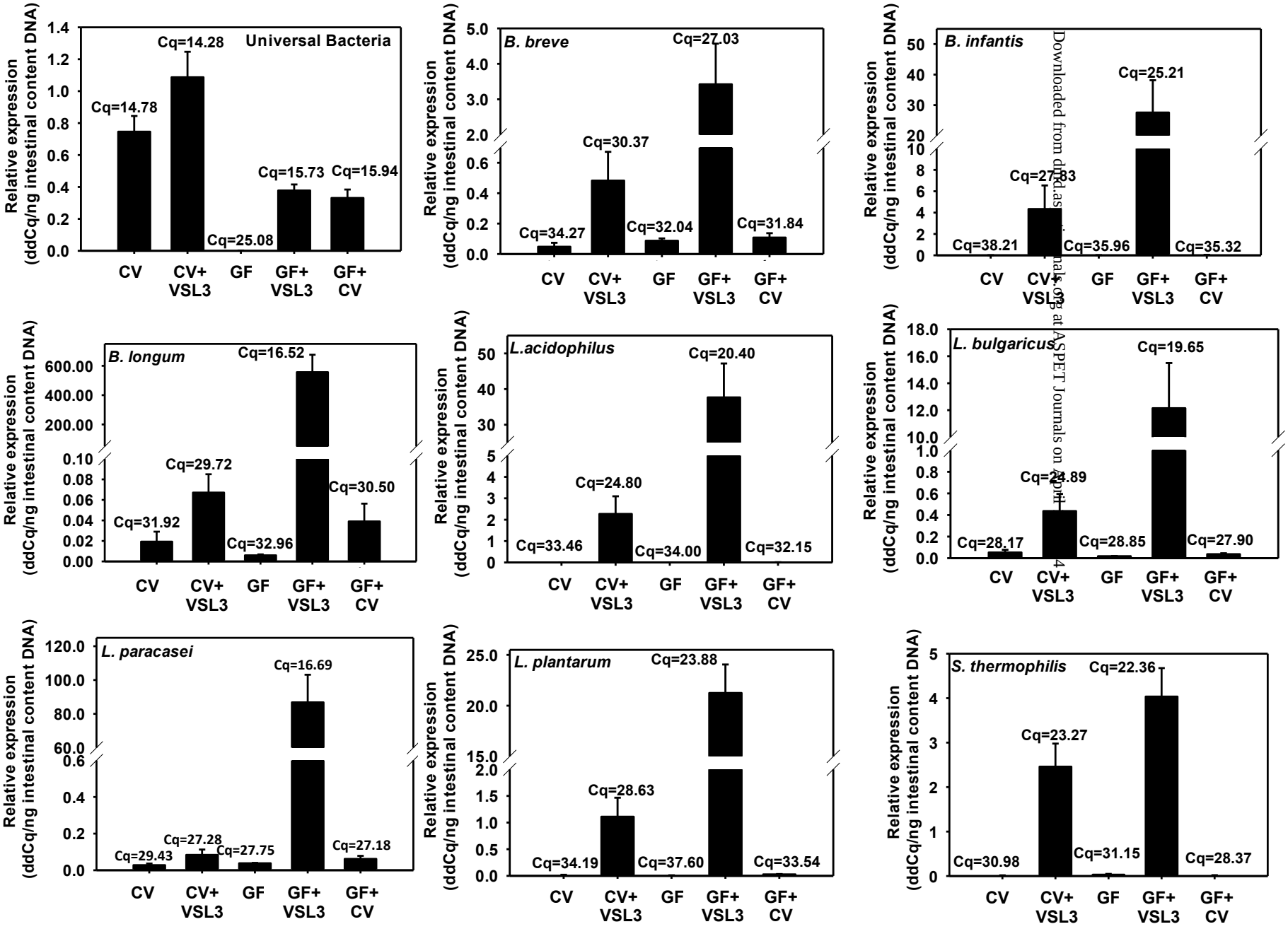

Figure 2

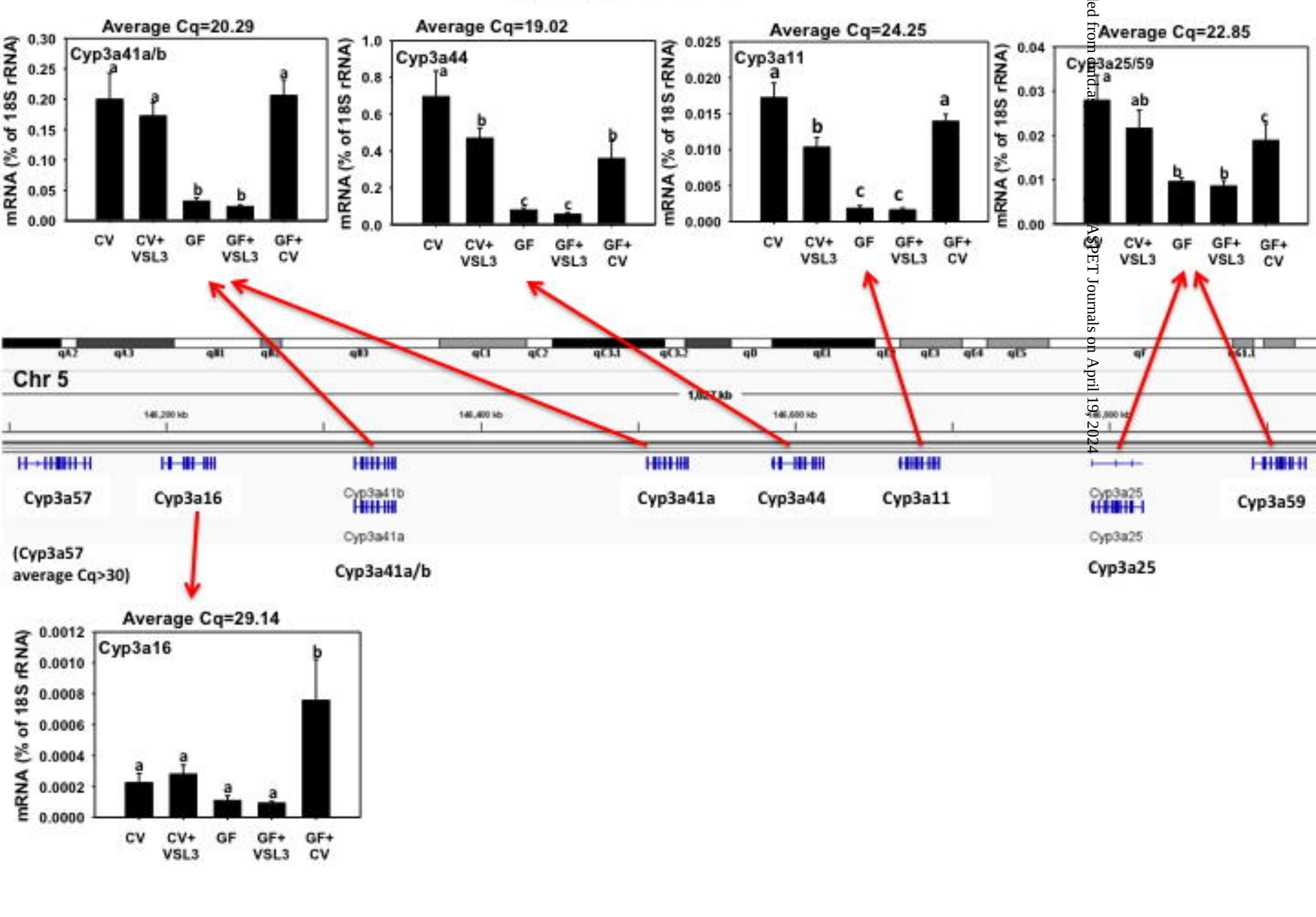

Figure 3

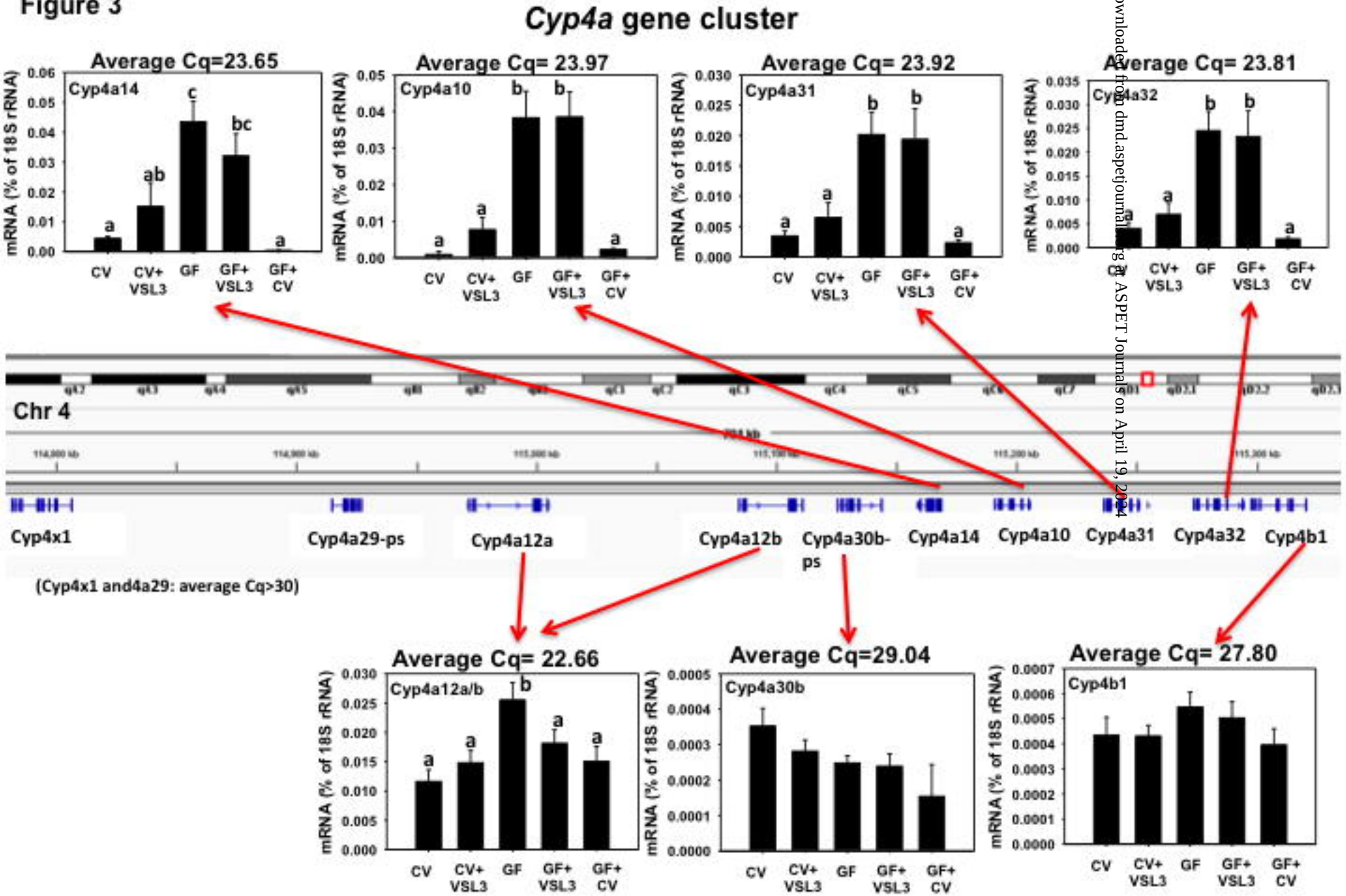

Figure 4

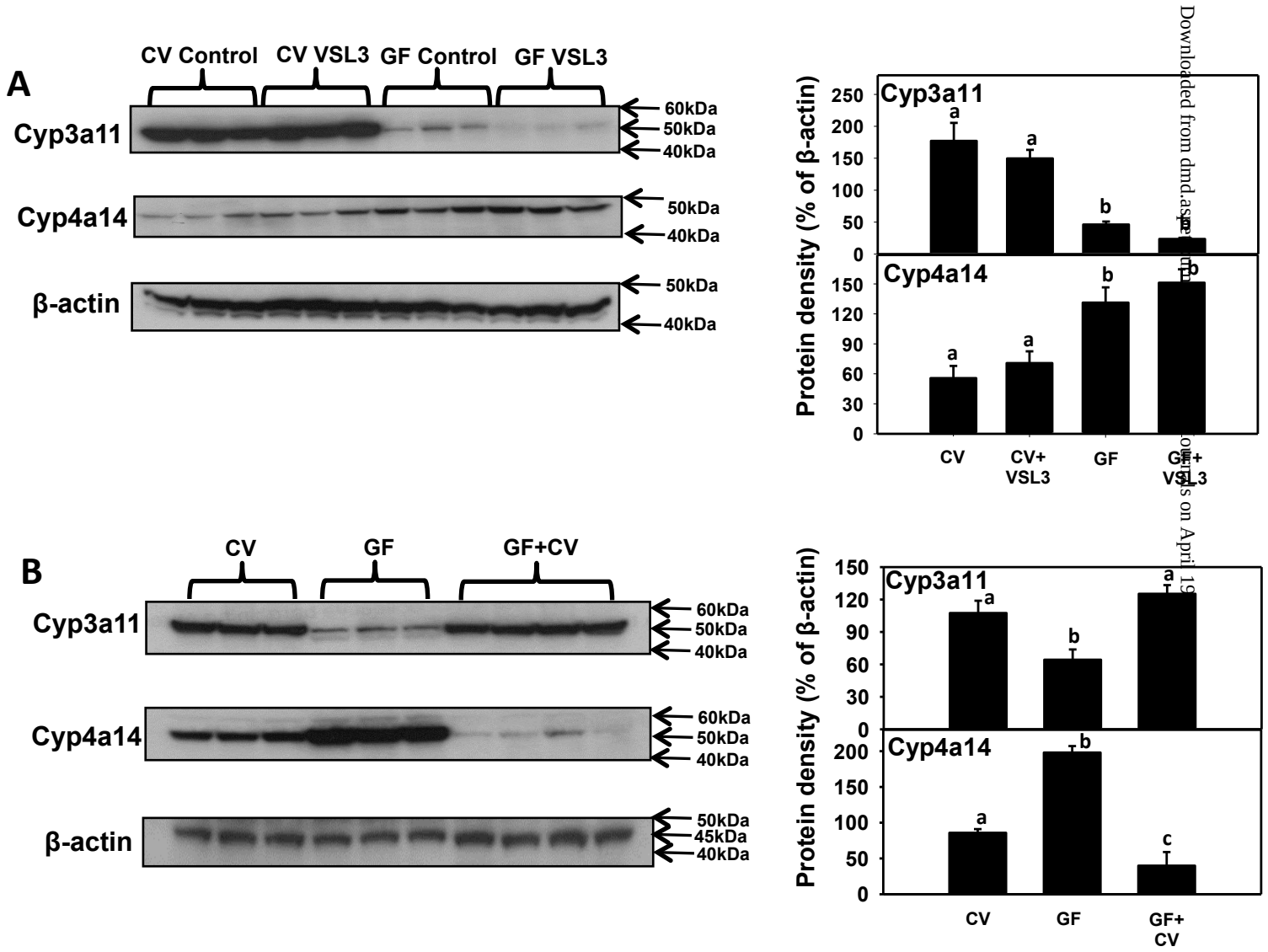

Figure 5

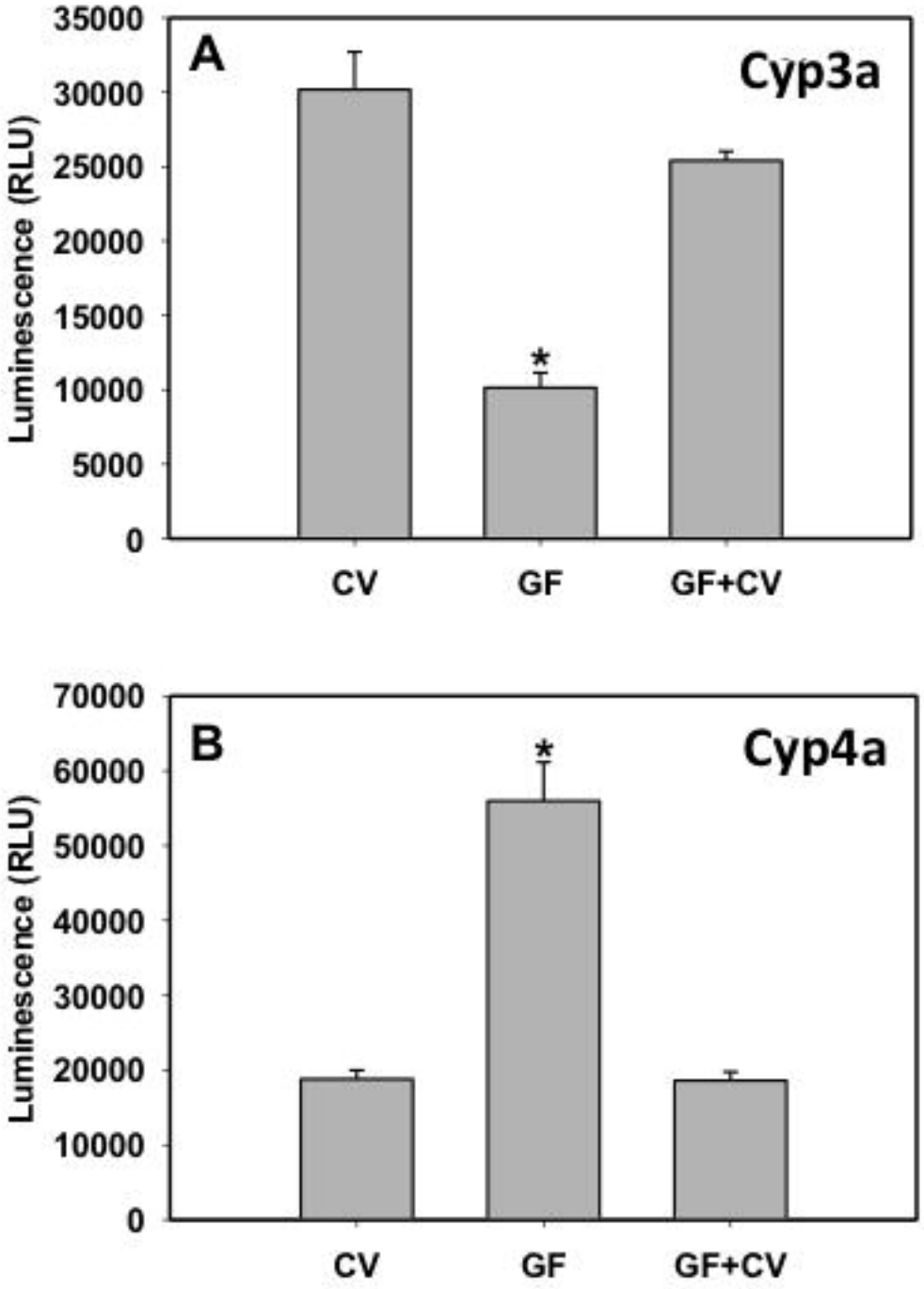

Figure 6

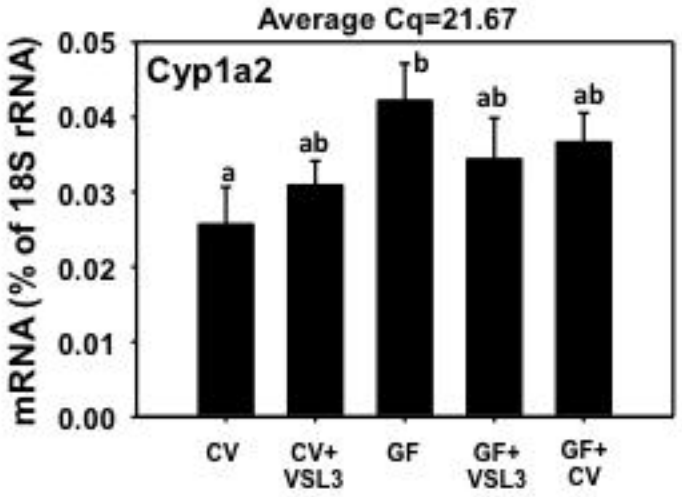

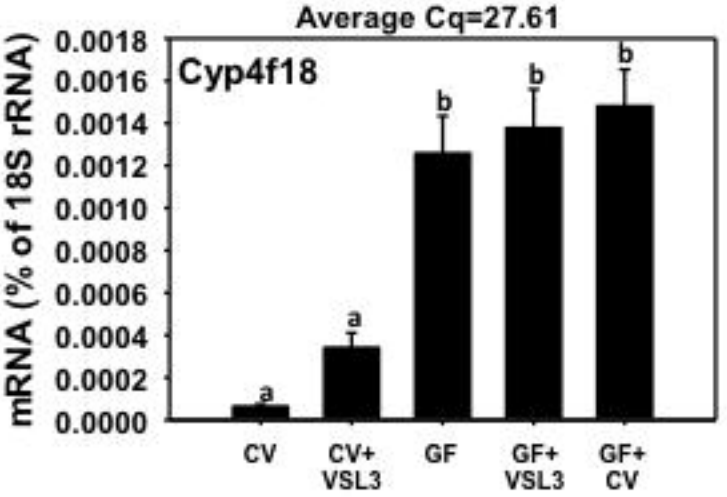

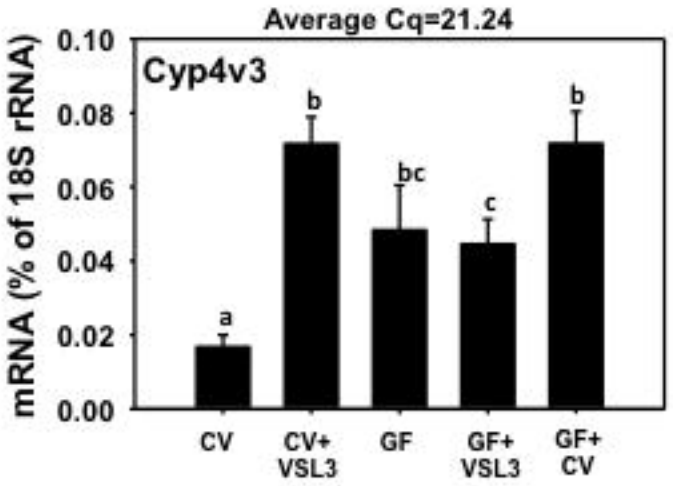

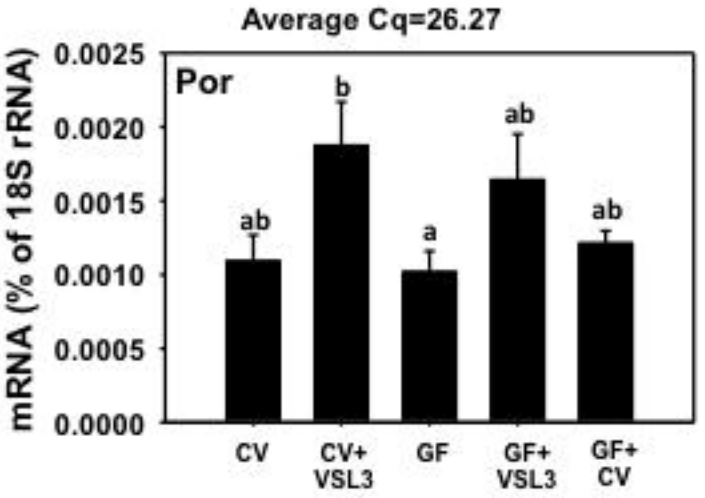

Figure 7

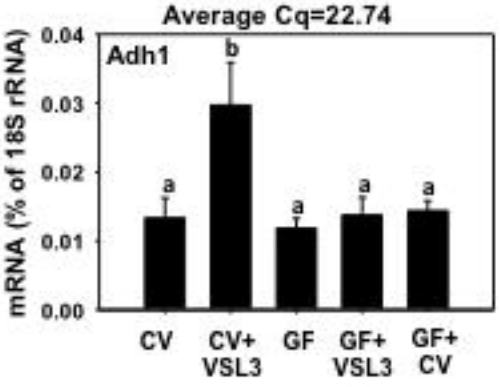

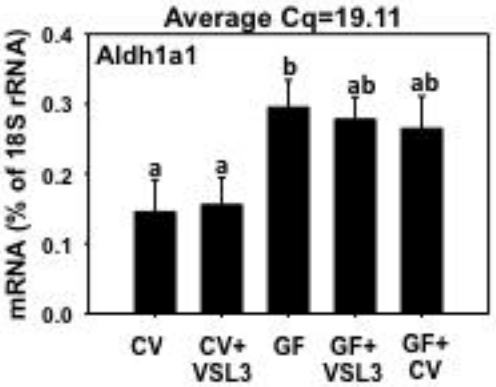

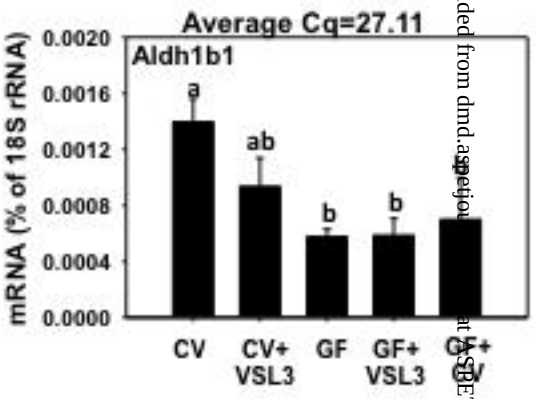

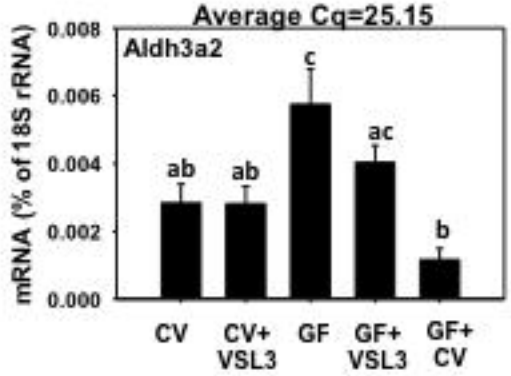

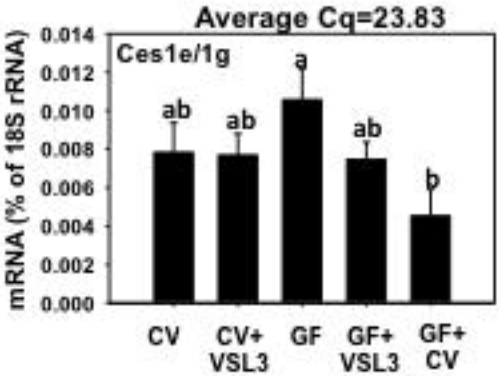

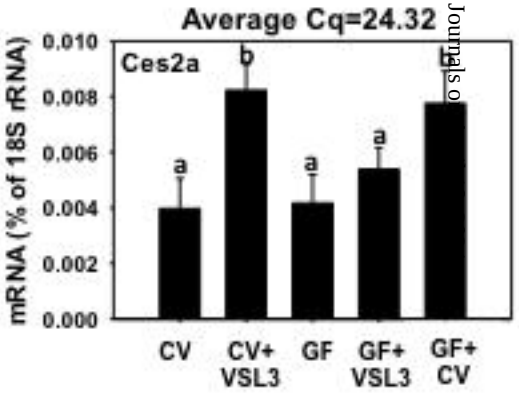

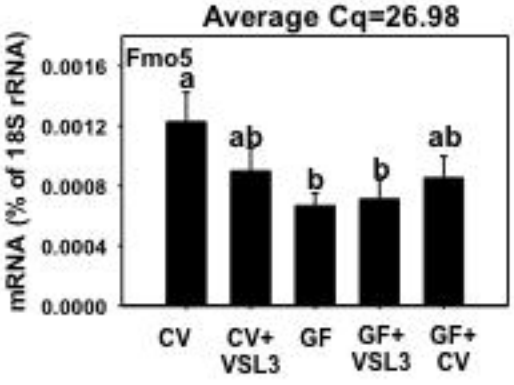

Figure 8

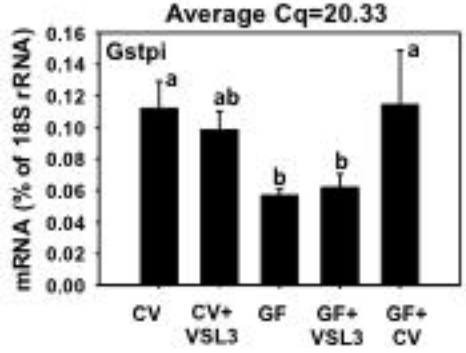

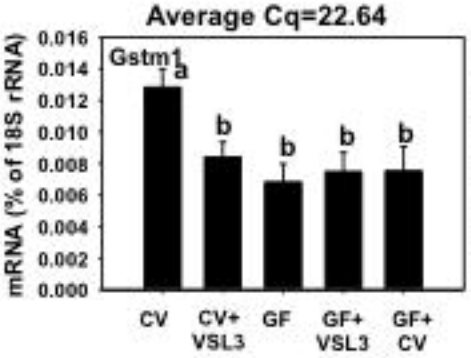

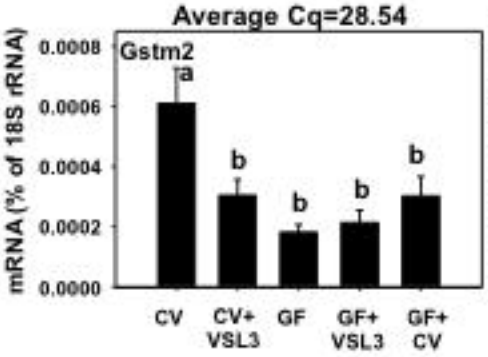

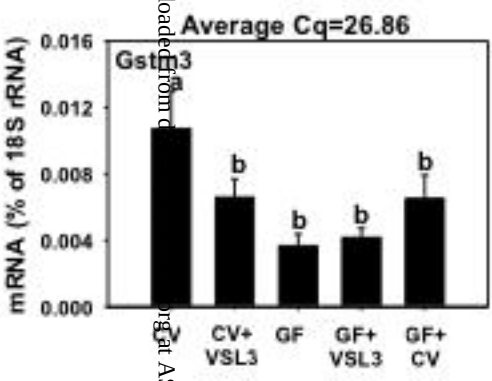

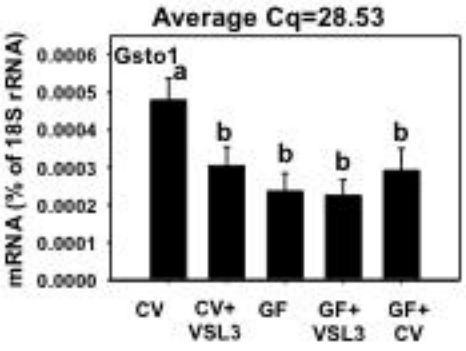

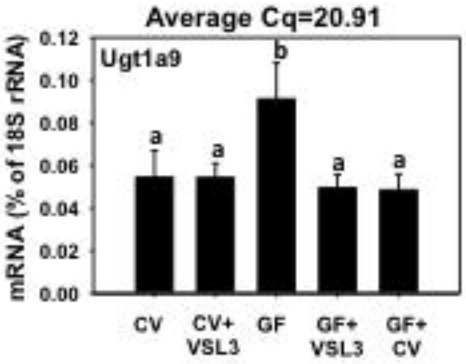

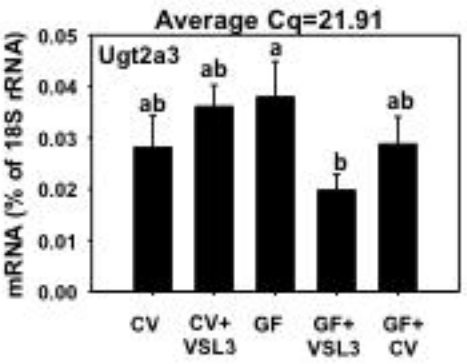

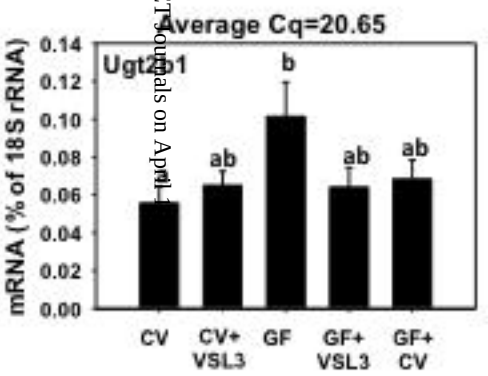

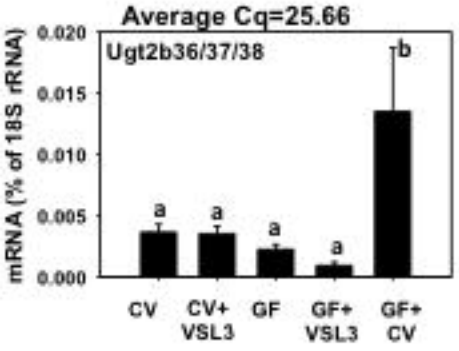

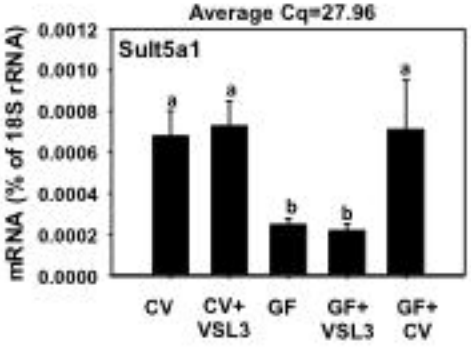

Figure 9

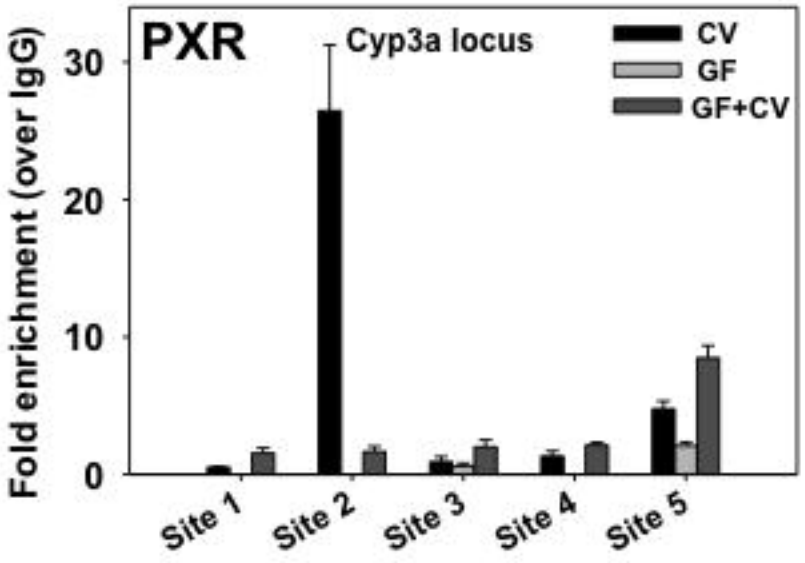

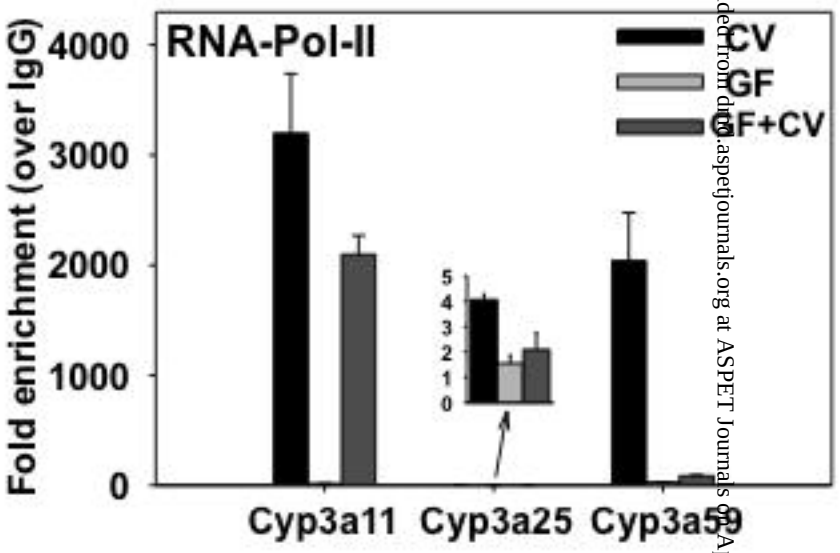

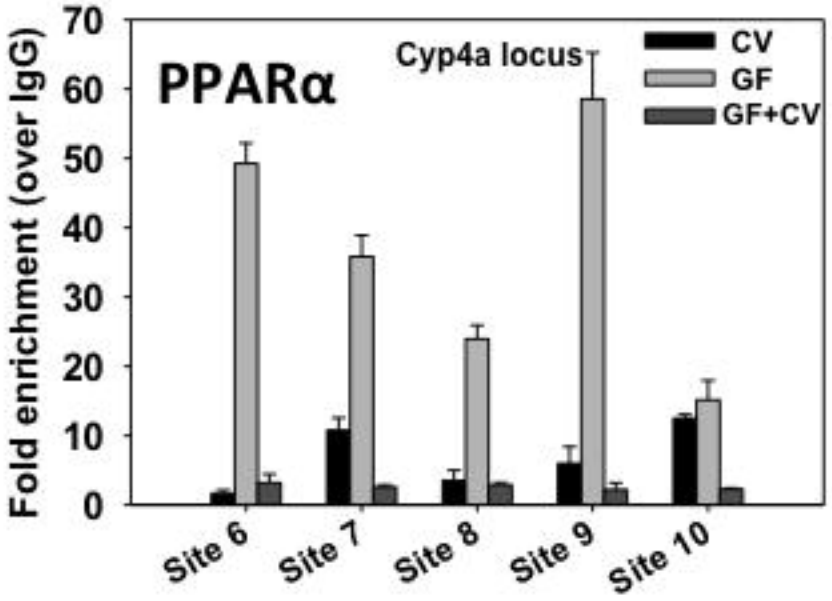

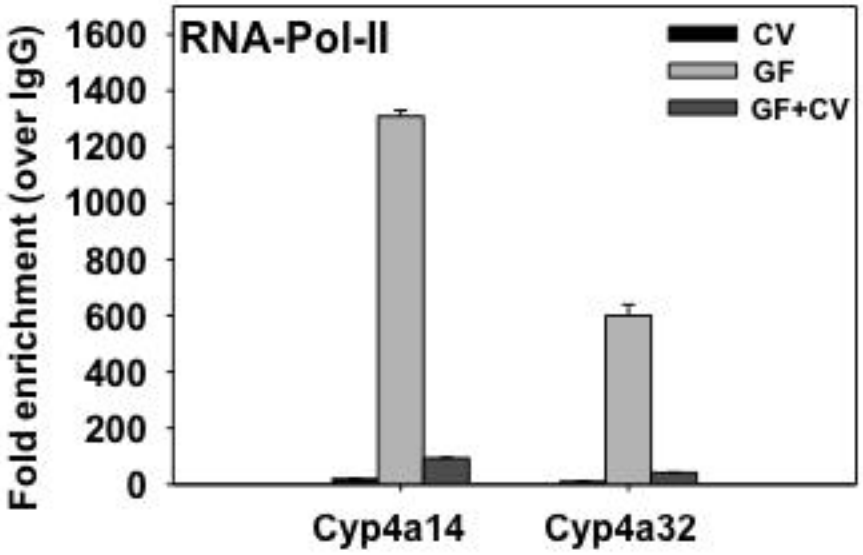

Supplemental Material:

Article title: Regulation of Hepatic Drug-metabolizing Enzymes in Germ-free mice by Conventionalization and Probiotics

Authors: Felcy Selwyn, Sunny Lihua Cheng, Curtis D. Klaassen, and Julia Yue Cui

Journal: Drug Metabolism and Disposition

Figure s1

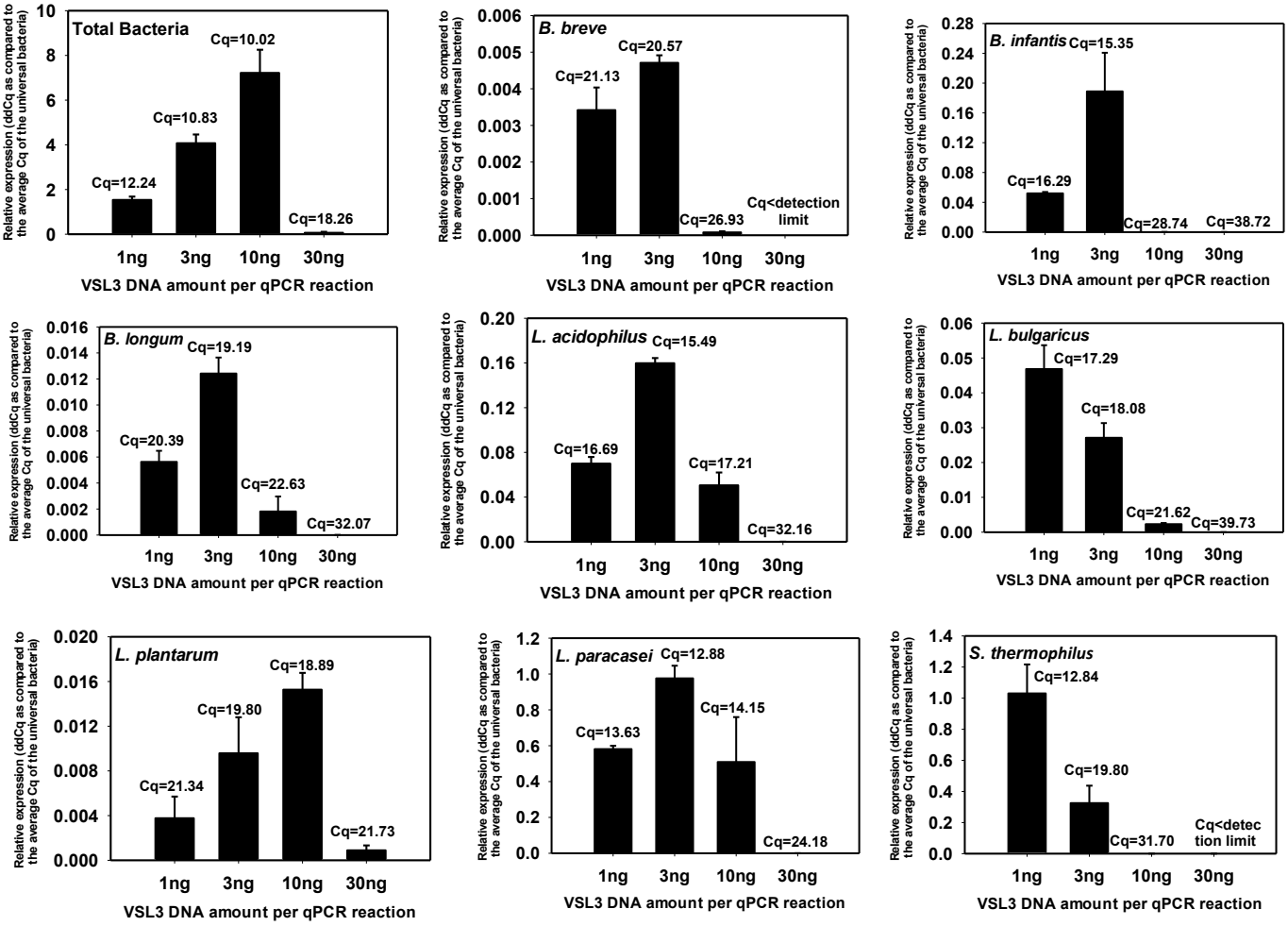
Total Bacteria
Cq=12.24
Cq=10.83
Cq=10.02
Cq=18.26
B. breve
Cq=21.13
Cq=20.57
Cq=26.93
Cq<detection limit
B. infantis
Cq=16.29
Cq=15.35
Cq=28.74
Cq=38.72
B. longum
Cq=20.39
Cq=19.19
Cq=22.63
Cq=32.07
L. acidophilus
Cq=16.69
Cq=15.49
Cq=17.21
Cq=32.16
L. bulgaricus
Cq=17.29
Cq=18.08
Cq=21.62
Cq=39.73
L. plantarum
Cq=21.34
Cq=19.80
Cq=18.89
Cq=21.73
L. paracasei
Cq=13.63
Cq=12.88
Cq=14.15
Cq=24.18
S. thermophilus
Cq=12.84
Cq=19.80
Cq=31.70
Cq<detection limit
1ng 3ng 10ng 30ng
VSL3 DNA amount per qPCR reaction
Relative expression (ddCq as compared to the average Cq of the universal bacteria)

Figure s2

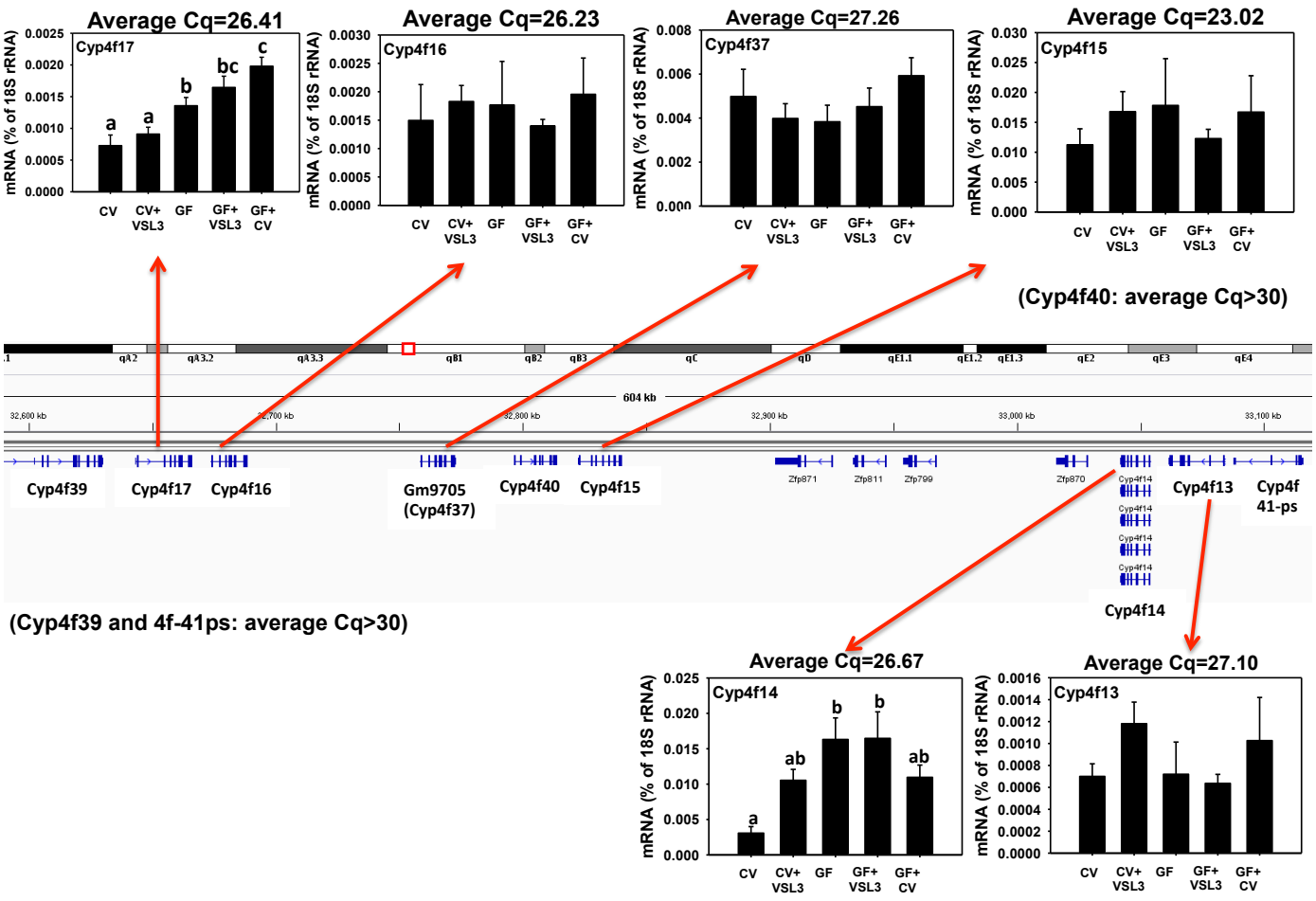
Cyp4f gene cluster
Average Cq=26.41
Cyp4f17
mRNA (% of 18S rRNA)
CV
CV+ VSL3
GF
GF+ VSL3
GF+ CV
Average Cq=26.23
Cyp4f16
Average Cq=27.26
Cyp4f37
Average Cq=23.02
Cyp4f15
(Cyp4f40: average Cq>30)
604 kb
Cyp4f39
Cyp4f17
Cyp4f16
Gm9705 (Cyp4f37)
Cyp4f40
Cyp4f15
Cyp4f13
Cyp4f 41-ps
Cyp4f14
(Cyp4f39 and 4f-41ps: average Cq>30)
Average Cq=26.67
Average Cq=27.10

Figure s3

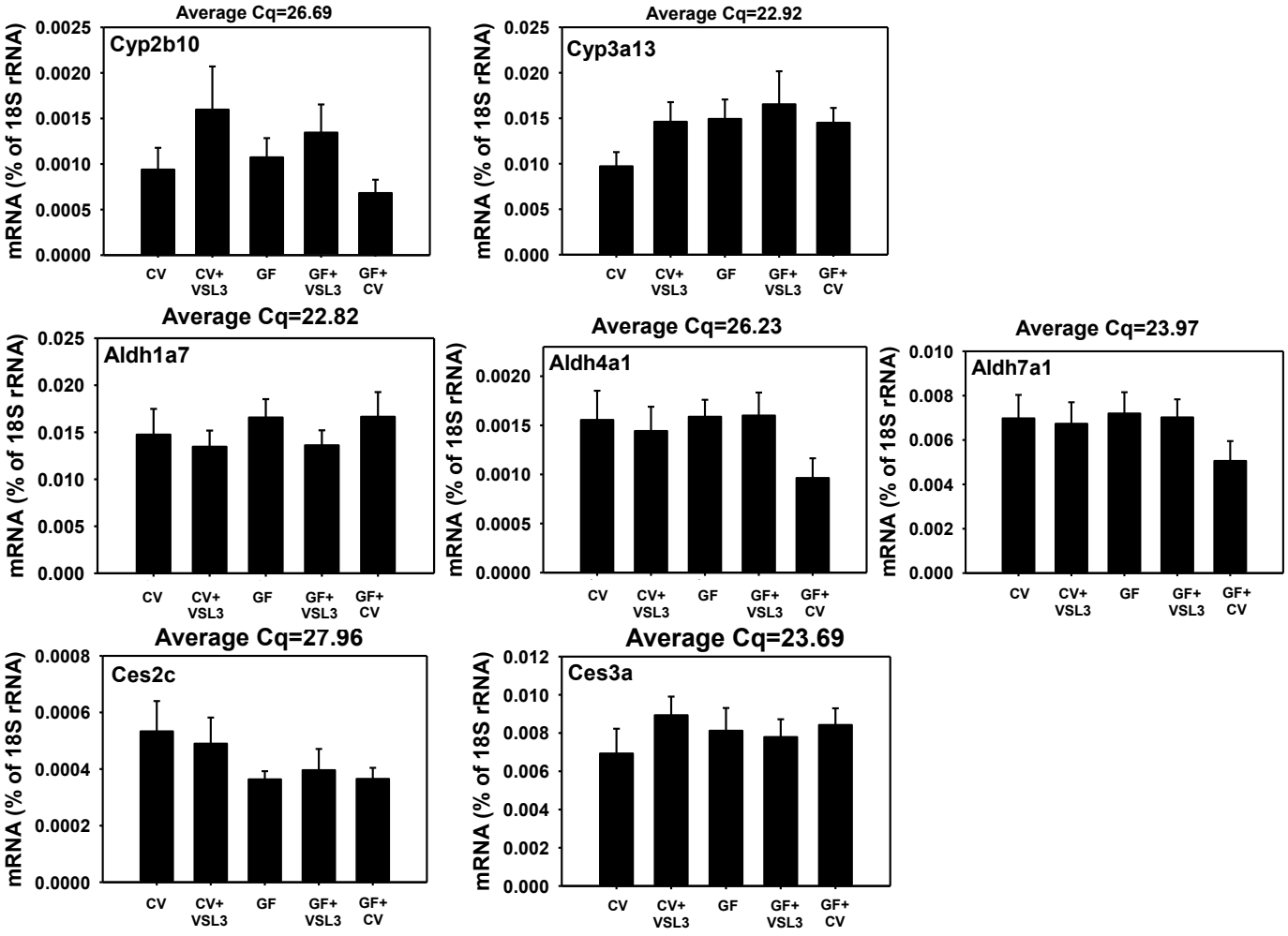
Average Cq=26.69
Cyp2b10
mRNA (% of 18S rRNA)
0.0025
0.0020
0.0015
0.0010
0.0005
0.0000
CV
CV+ VSL3
GF
GF+ VSL3
GF+ CV
Average Cq=22.92
Cyp3a13
0.025
0.020
0.015
0.010
0.005
0.000
Average Cq=22.82
Aldh1a7
Average Cq=26.23
Aldh4a1
0.0020
0.0015
0.0010
0.0005
0.0000
Average Cq=23.97
Aldh7a1
0.010
0.008
0.006
0.004
0.002
0.000
Average Cq=27.96
Ces2c
0.0008
0.0006
0.0004
0.0002
0.0000
Average Cq=23.69
Ces3a
0.012
0.010
0.008
0.006
0.004
0.002
0.000

Figure s4

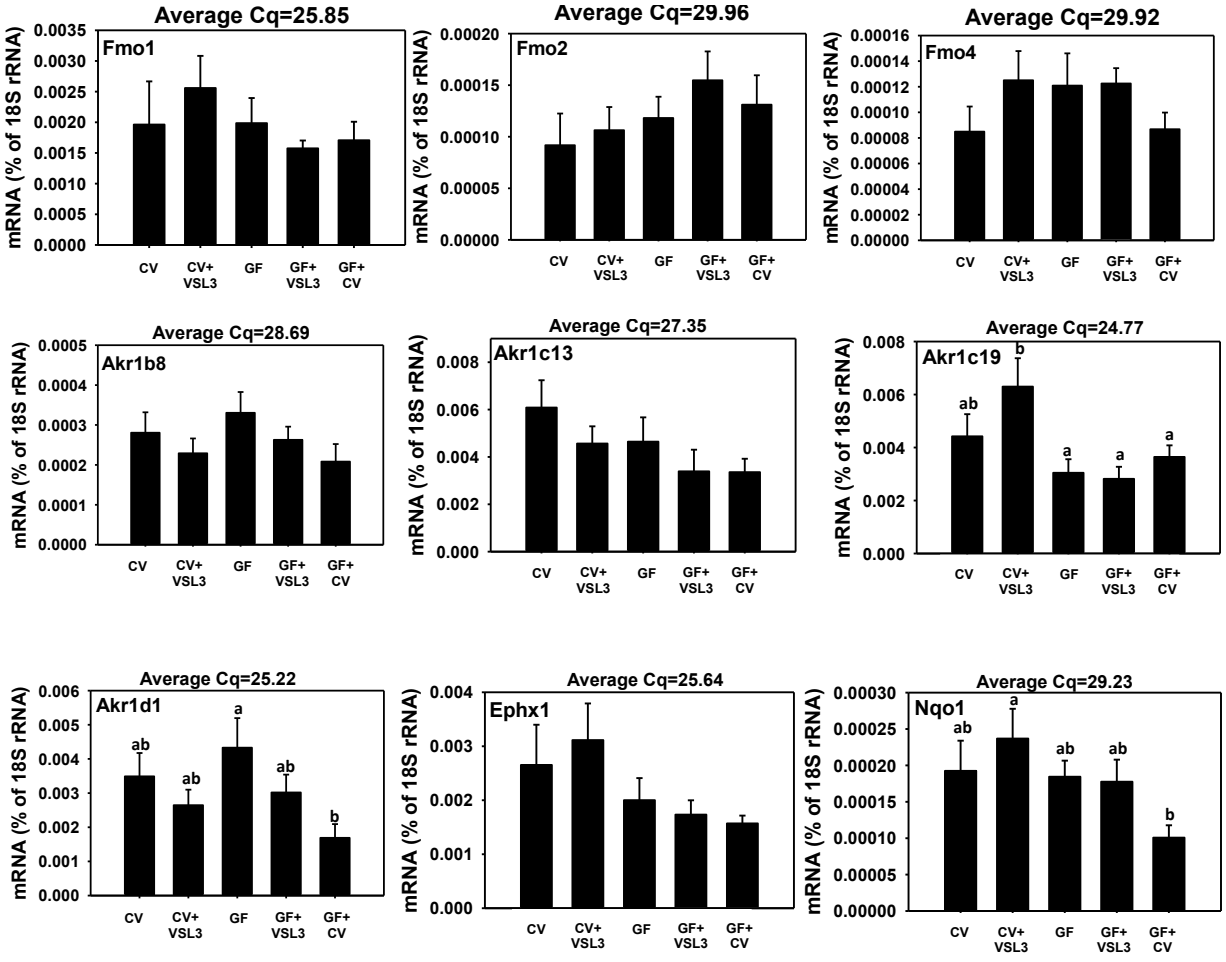
Average Cq=25.85
Fmo1
mRNA (% of 18S rRNA)
0.0035
0.0030
0.0025
0.0020
0.0015
0.0010
0.0005
0.0000
CV
CV+ VSL3
GF
GF+ VSL3
GF+ CV
Average Cq=29.96
Fmo2
mRNA (% of 18S rRNA)
0.00020
0.00015
0.00010
0.00005
0.00000
CV
CV+ VSL3
GF
GF+ VSL3
GF+ CV
Average Cq=29.92
Fmo4
mRNA (% of 18S rRNA)
0.00016
0.00014
0.00012
0.00010
0.00008
0.00006
0.00004
0.00002
0.00000
CV
CV+ VSL3
GF
GF+ VSL3
GF+ CV
Average Cq=28.69
Akr1b8
mRNA (% of 18S rRNA)
0.0005
0.0004
0.0003
0.0002
0.0001
0.0000
CV
CV+ VSL3
GF
GF+ VSL3
GF+ CV
Average Cq=27.35
Akr1c13
mRNA (% of 18S rRNA)
0.008
0.006
0.004
0.002
0.000
CV
CV+ VSL3
GF
GF+ VSL3
GF+ CV
Average Cq=24.77
Akr1c19
mRNA (% of 18S rRNA)
0.008
0.006
0.004
0.002
0.000
ab
b
a
a
a
CV
CV+ VSL3
GF
GF+ VSL3
GF+ CV
Average Cq=25.22
Akr1d1
mRNA (% of 18S rRNA)
0.006
0.005
0.004
0.003
0.002
0.001
0.000
ab
ab
a
ab
b
CV
CV+ VSL3
GF
GF+ VSL3
GF+ CV
Average Cq=25.64
Ephx1
mRNA (% of 18S rRNA)
0.004
0.003
0.002
0.001
0.000
CV
CV+ VSL3
GF
GF+ VSL3
GF+ CV
Average Cq=29.23
Nqo1
mRNA (% of 18S rRNA)
0.00030
0.00025
0.00020
0.00015
0.00010
0.00005
0.00000
ab
a
ab
ab
b
CV
CV+ VSL3
GF
GF+ VSL3
GF+ CV

Figure s5

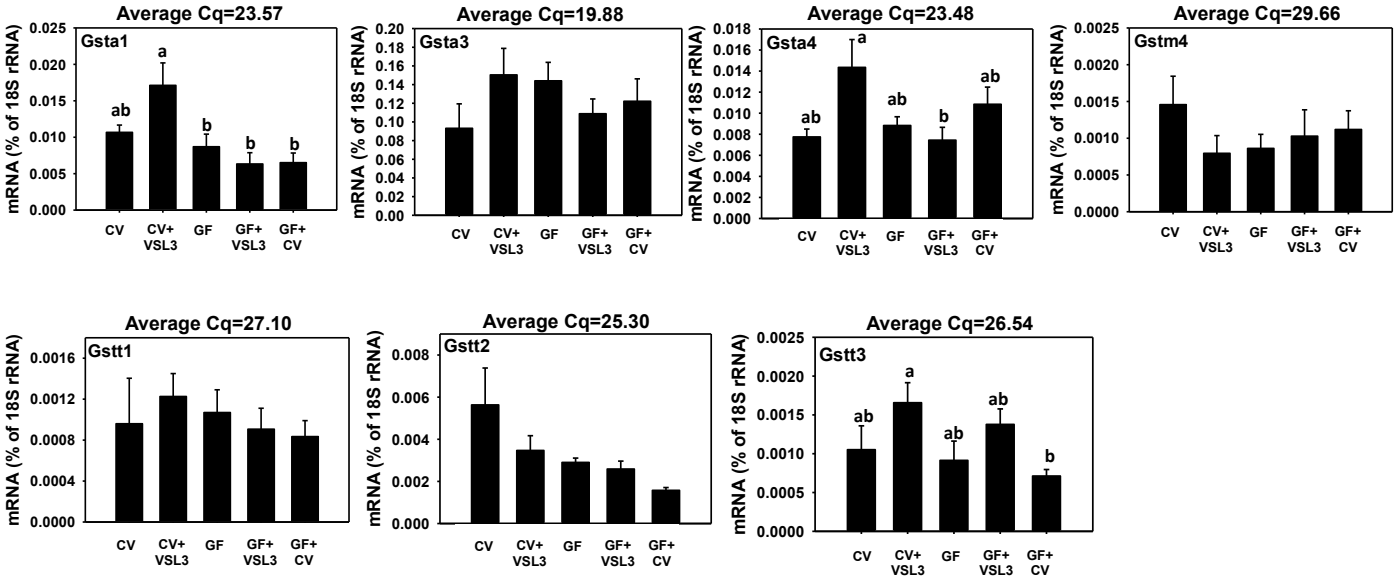
Average Cq=23.57
Gsta1
mRNA (% of 18S rRNA)
0.025
0.020
0.015
0.010
0.005
0.000
a
ab
b
b
b
CV
CV+ VSL3
GF
GF+ VSL3
GF+ CV
Average Cq=19.88
Gsta3
mRNA (% of 18S rRNA)
0.20
0.18
0.16
0.14
0.12
0.10
0.08
0.06
0.04
0.02
0.00
CV
CV+ VSL3
GF
GF+ VSL3
GF+ CV
Average Cq=23.48
Gsta4
mRNA (% of 18S rRNA)
0.018
0.016
0.014
0.012
0.010
0.008
0.006
0.004
0.002
0.000
a
ab
ab
b
ab
CV
CV+ VSL3
GF
GF+ VSL3
GF+ CV
Average Cq=29.66
Gstm4
mRNA (% of 18S rRNA)
0.0025
0.0020
0.0015
0.0010
0.0005
0.0000
CV
CV+ VSL3
GF
GF+ VSL3
GF+ CV
Average Cq=27.10
Gstt1
mRNA (% of 18S rRNA)
0.0016
0.0012
0.0008
0.0004
0.0000
CV
CV+ VSL3
GF
GF+ VSL3
GF+ CV
Average Cq=25.30
Gstt2
mRNA (% of 18S rRNA)
0.008
0.006
0.004
0.002
0.000
CV
CV+ VSL3
GF
GF+ VSL3
GF+ CV
Average Cq=26.54
Gstt3
mRNA (% of 18S rRNA)
0.0025
0.0020
0.0015
0.0010
0.0005
0.0000
ab
a
ab
ab
b
CV
CV+ VSL3
GF
GF+ VSL3
GF+ CV

Figure s6

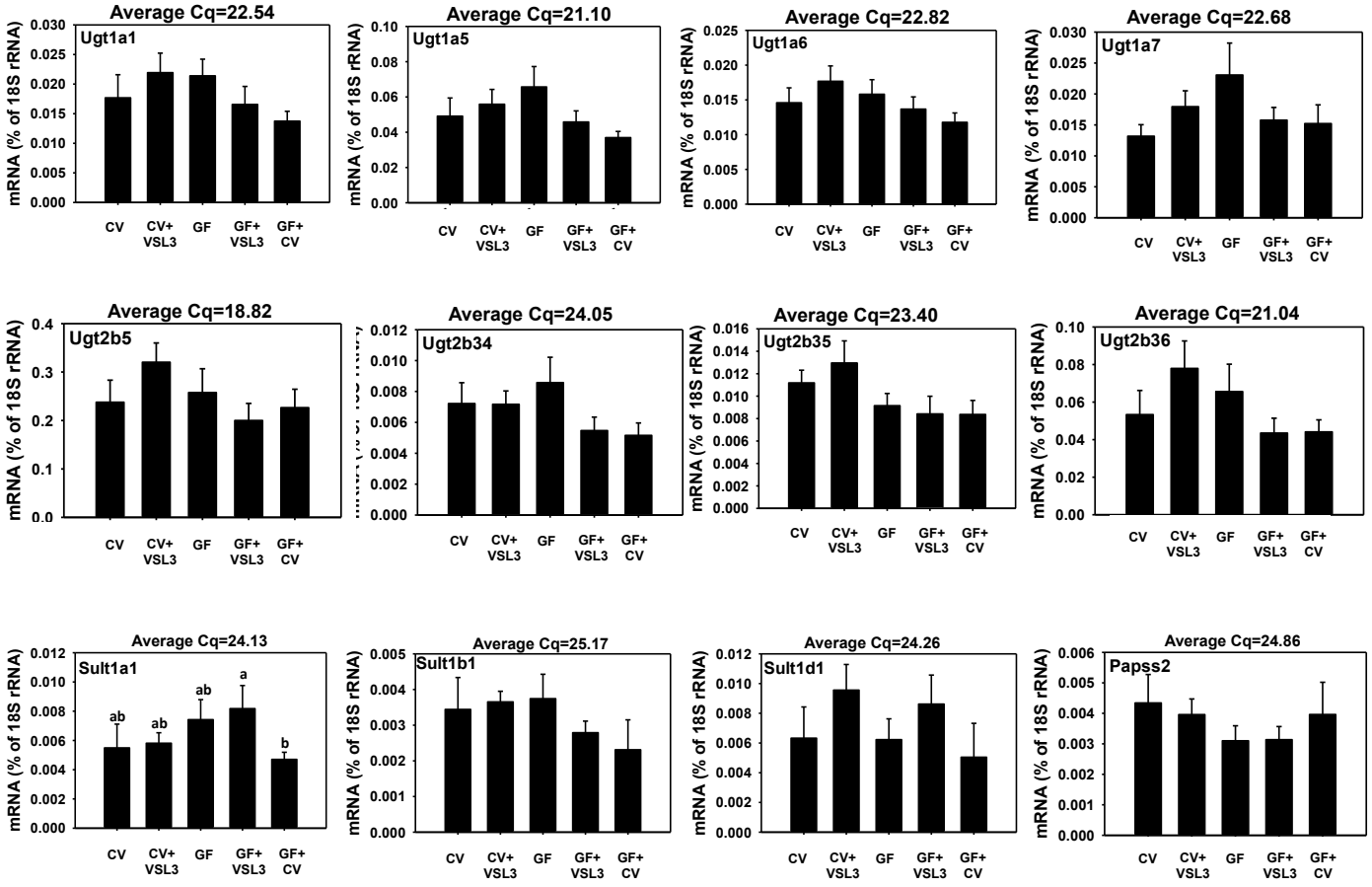
Average Cq=22.54
Ugt1a1
Average Cq=21.10
Ugt1a5
Average Cq=22.82
Ugt1a6
Average Cq=22.68
Ugt1a7
Average Cq=18.82
Ugt2b5
Average Cq=24.05
Ugt2b34
Average Cq=23.40
Ugt2b35
Average Cq=21.04
Ugt2b36
Average Cq=24.13
Sult1a1
ab
ab
ab
a
b
Average Cq=25.17
Sult1b1
Average Cq=24.26
Sult1d1
Average Cq=24.86
Papss2
mRNA (% of 18S rRNA)
CV
CV+ VSL3
GF
GF+ VSL3
GF+ CV

Figure s7

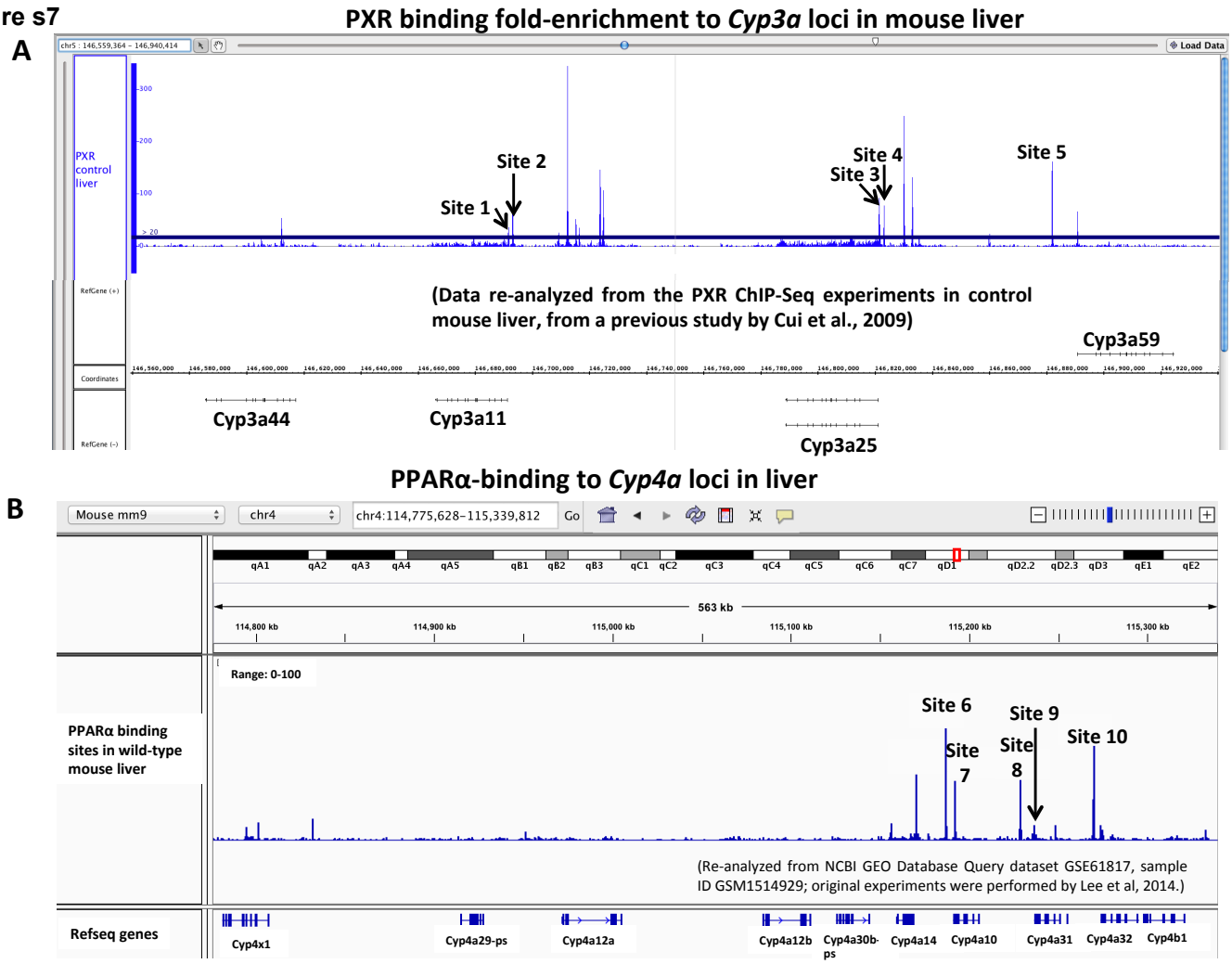
A
PXR binding fold-enrichment to *Cyp3a* loci in mouse liver
Load Data
PXR control liver
Site 1
Site 2
Site 3
Site 4
Site 5
(Data re-analyzed from the PXR ChIP-Seq experiments in control mouse liver, from a previous study by Cui et al., 2009)
Cyp3a59
Cyp3a44
Cyp3a11
Cyp3a25
B
PPARα-binding to *Cyp4a* loci in liver
Mouse mm9
chr4
chr4:114,775,628-115,339,812
Go
563 kb
Range: 0-100
PPARα binding sites in wild-type mouse liver
Site 6
Site 7
Site 8
Site 9
Site 10
(Re-analyzed from NCBI GEO Database Query dataset GSE61817, sample ID GSM1514929; original experiments were performed by Lee et al, 2014.)
Refseq genes
Cyp4x1
Cyp4a29-ps
Cyp4a12a
Cyp4a12b
Cyp4a30b-ps
Cyp4a14
Cyp4a10
Cyp4a31
Cyp4a32
Cyp4b1

Table s1. Primer Sequences and Specificity for the bacterial 16S rRNA quantification.

Bacterial 16S rRNA targeted	Primer sequences	Cross-reactivity
Universal bacteria	Forward: GTGSTGCAYGGYTGTCGTCA	Universal
	Reverse: ACGTCRTCCMCACCTTCCTC	
L. acidophilus	Forward: AGCGAGCTGAACCAACAGAT	***L. acidophilus*** NBRC13951, VPI6032, JCM1132, and BCRC10695 strains.
	Reverse: TGATCATGCGATCTGCTTTC	***L. acidophilus*** strains NCFM, NBRC 13951, VPI 6032, JCM 1132, and BCRC 10695; ***L. crispatus*** strains DSM 20584, ST1, NBRC 15019, ATCC 33820; ***L. helveticus*** strains DPC 4571, NBRC 15019, DSM 20075; ***L. gallinarum*** strainsATCC 33199, JCM 2011; ***L. ultunesis*** strains CCUG 48460, Kx146C1; ***L. kitasatonis*** strain JCM 1039.
L. plantanum	Forward: TTTGAGTGAGTGGCGAACTG	***L. plantarum*** strains CIP WCFS1, CIP 103151, NBRC 15891, JCM 1149, NRRL B-14768, subsp. argentoratensis strain DKO22, DSM 10667, JCM 1149; ***L. paraplantarum*** strain DSM 10667; ***L. mudanjiangensis*** strain 11050; ***L. fabifermentans*** strains DSM 21115, LMG 24284; ***L. xiangfangensis*** strain 3.1.1; ***L. pentosus*** strain 124-2.
	Reverse: CCAAAAGTGATAGCCGAAGC	***L. plantarum*** strains WCFS1, CIP 103151, NBRC 15891, JCM 1149, NRRL B-14768, subsp. argentoratensis strain DKO 22; ***L. paraplantarum*** strain DSM 10667; ***L. xiangfangensis*** strain 2.1.1; ***L. pentosus*** strain 124-2.
B. longum	Forward: TTTTGTGGAGGGTTCGATTC	***B. longum*** strains subsp. suis strain ATCC 227533, ATCC 15707; NCC2705 strain NCC2705; ***B. bifidum*** S17 strain S17; B. breve ACS-0710V Sch8b strain ACS-071-V-Sch8b; ***B. animalis*** subsp. Lactis AD011 strain AD011; ***B. adolescentis*** strain ATCC15703
	Reverse: GGAGCTATTCCGGTGTATGG	***B. longum*** strains subsp. Suis strain ATCC 27533, ATCC15070, NCC2705 strain NCC2705, KCTC3128, subsp. Infantis strain ATCC 15697; ***B. dentium*** strain B764, Bd1 strain Bd1, ***B. moukalabense*** strain GG01; ***B. stercoris*** strain Eg1; ***B. adolescentis*** strain ATCC15703; ***B. pseudocatenulatum*** strain B1279; ***B. catenulatum*** strain DSM 16992; ***B. ruminantium*** strain Ru 687; ***B. indicum*** strain JCM1302.
B. breve	Forward: CTGAGATACGGCCCAGACTC	Many including ***B. breve*** strains
	Reverse: ACAAAGTGCCTTGCTCCCTA	***B. breve*** strains DSM 20213 and ACS-071-V-Sch8b strain ACS-071-V-Sch8b
L. paracasei	Forward: CGAGATTCAACATGGAACGA	***L. paracasei*** strains ATCC334 strain ATCC 334, NBRC 15889, ATCC25302, subsp. Tolerans strain NBRC 15906, R094
	Reverse: AGCTTACGCCATCTTTCAGC	***L. paracasei*** strains NBRC 15889, ATCC 25302, subsp. Tolerans strain NBRC 15906, R094; ***L. rhamnosus*** GG strain GG (ATCC 53103), NBRC 3425, JCM 1136; ***L. casei*** ATCC 334 strain ATCC 334; ***L. saniviri*** strain YIT 12363; ***L. zeae*** strain RIA 482
L. bulgaricus	Forward: CAAGTTTGAAAGGCGGCGTA	***L. delbrueckii subsp. Bulgaricus*** strains ATCC 11842, NBRC 13953, ATCC 11842
	Reverse: TTGCTCCATCAGACTTGCGT	Many including ***L. delbruieckii subsp. Bulgaricus strains***

Table S2 RT-qPCR primer sequences

Gene Symbol	Forward	Reverse
18S	CGAACGTCTGCCCTATCAACTT	CCGGAATCGAACCCTGATT
Adh1	GTTGAGAGCGTTGGAGAAGG	TCGCTTCGGCTACAAAAGTT
Akr1b8	TCCTCTTTGCTGATGCACAC	GCAACAGTCTGTCCCTGGTT
Akr1c13	CCTTCCAGCAGAGTTCCTTG	ACTGTCCACACACAGGGACA
Akr1c19	TTGCCTACTGTGCTCTTGGA	CAATCTGAGCTGGACTTCGC
Akr1d1	GAGTGCCACCCGTATTTCAC	CAAGGGTGGAGAAGAGACGT
Aldh1a1	CTCTGTTCCCCAGGTGTTGT	CATGCAAGGGTGCCTTTATT
Aldh1a7	TGCTATTTGGCTGTCCCTGT	ACCATGTTCGCCCAGTTCTC
Aldh1b1	GAACGATCAGTGAAGGACGC	CAACTGTGTCCATTGCCCAA
Aldh3a1	CCCCTGGCACTCTATGTGTT	GTGGGCACAGTGATGTGAAC
Aldh3a2	CACCACCCAAAGTCTGTGTG	AAGATGCTCTGAGTGGCCTT
Aldh4a1	GGAAGGAGACAGCTCTGGTG	GGAGCTAGCACAGACCAAGG
Aldh7a1	TGAAGAAACCATCGGGAAAG	TTCCCCATCTCCAAAGACAC
Ces1e/1g	TTGCTGGCTGTAAAACCACC	CTTTGGCAGCAACACTCCAT
Ces2a	GTACTGGGCCAATTTCGCAA	GTCCTGAGAACCCTTGAGCT
Ces2c	AGGAATGGCTTCCATGTTTG	AGGTATCCCCAGTTGCCTCT (also recognizes Ces2a and Ces2h)
Ces3a	CACAGACCGCATGGTAATTG	TTGATGCTGGCATCTCTCAC
Cyp1a2	GACATGGCCTAACGTGCAG	GGTCAGAAAGCCGTGGTTG
Cyp2b10	AAGGAGAAGTCCAACCAGCA	CTCTGCAACATGGGGGTACT
Cyp3a11	ACAAACAAGCAGGGATGGAC	GGTAGAGGAGCACCAAGCTG
Cyp3a13	AAGTACTGGCCAGAGCCTGA	AATGCAGTTCCTTGGTCCAC
Cyp3a16	GTATGAAACCACCAGCAGCA	AGGTATTCCATCGCCATCAC
Cyp3a41a/b	AGCAGAAGCACCGAGTTGAT	GACTGGGCTGTGATCTCCAT
Cyp3a44	CTGAGCTTTCTCAGTGTCTGTGCA	CCCATGAGAAACGGTGAAGGCA
Cyp3a57	TCTATCCTCTTCATCGGGACCCCG	GGTTGCCTGCTGATCTTCACAGGG
Cyp3a59/25	AGTACTGGCCAGAGCCTCAA	TCGTTCTCCTTGCTGAACCT
Cyp4a10	CACACCCTGATCACCAACAG	TCCTTGATGCACATTGTGGT
Cyp4a12a/b	CTCATTCCTGCCCTTCTCAG	GGTATGGGGATTGGGACTCT
Cyp4a14	CTGGGTGATGGAACCTCTGT	CATCTGGGAAGGTGACAGGT
Cyp4a29	TGATGGGAGCAGCTTGTCTG	GGTCGGGATGTGTAGCCAAA
Cyp4a30b	GGTGATACTGGGGCGATCAG	GAGGGCAATCTTGGTCCACA
Cyp4a31	TGCAGGCAGCCTCTCTGGCT	GGGCGGTGATGGGAACTGCT
Cyp4a32	TCTGCTCTAAGCCCGACCCGA	GCAGCAGGAGCAGACCGAGC
Cyp4b1	CTGCATGGCCCTTTATCCTA	GAAGCACTCCTTCATGCACA
Cyp4f13	TATCTCACTGCTGATGGGCG	AGGAATTCAACACCCTGCGT
Cyp4f14	GTCACGTGGGCATGGTAACT	TCGGACGATGTCAGAATGGC
Cyp4f15	GACAGGGAACCAGCAGTTGT	ATCCTGCCTAGACACTTCCCT
Cyp4f16	GGCAGAGGCTGACACCTTTA	ATCTCCTCAGGCTCTCGGTC
Cyp4f17	TGATGACCTTGGACAGCTTG	AAGGTACAGGAAGGGCTGGT
Cyp4f18	GAGGAGATTGAATGGGACGA	GGGAGCACAATGTCCTGAGT
Cyp4f37	ACTGAAGCAGGCCAGACTTACCG	GGGGGCAACAAATGCAGGGTCA
Cyp4f39	GACTTCCGCATTACCTGTCG	AGAAAGGTCCAACCCATGCC
Cyp4f40	GGCTGTGAAGAGAAACGAGC	GGCATCGGTGAAGTCGTGTA
Cyp4v3	TCCGAGTTTTCCCATCTGTC	CGGTGTAGTGCGTAGGGAAT
Cyp4x1	TGGTCCAAGGAACTGCATCG	TGGTGAGGTCTGGAGCTACT
Cypy4f41-ps	AGAACTGAGTTATCAGGTTCAGC	GTCACCTGGAAGTCTGACCG
Ephx1	AGGCATCCAGCAAGAAAGGT	AGATGAGAGACCCCCAGTCG
Fmo1	AAACAAGCATAGCGGGTTTG	ATCCGGTTTTGCGTTGATAG
Fmo2	AATGGCAAAGAAGGTTGTGG	TCAGTCCTTTCGAAGCAGGT
Fmo3	GGGGGAAAAGTTCAAATGGT	CCTGGGATCCTTGAGAAACA
Fmo4	CGCCCAGACTTCTCTGAAAC	AAATGTGGGCTCAGGAATTG
Fmo5	ACAGGGCTCTGAGTCAGCAT	CCTGGAGCCATCCTCAAATA
Fmo6	ACTGAAAAGGAAGGCAAGCA	GTAGGCACTTGCCTCGAAAG
Fmo9	GAGGAGCGTGAGAAAACGTC	AAGGACTTGAGTGGCAGGTG
Gsta1	CGCCACCAAATATGACCTCT	TTGCCCAATCATTTCAGTCA
Gsta3	TACTTTGATGGCAGGGGAAG	GCACTTGCTGGAACATCAGA
Gsta4	TGATGATGATTGCCGTGGCT	ACGAGAAAAGCCTCTCCGTG
Gstm1	CTCCCGACTTTGACAGAAGC	TTGCTCTGGGTGATCTTGTG
Gstm2	ATGGTTTGCAGGGAACAAGGT	CTTCAGGCCCTCAAAGCGAC
Gstm3	AGAGGAGGAGAGGATCCGTG	GGGACTGCAGCAGACTATCAT
Gstm4	TATGACACTGGGTTACTGGGACATC	TCCACGCGAATCTTCTCTTCC
Gsto1	ATTGATGCCAAGACCTACCG	CAGTGAGGGGAAACAGCATT
Gstpi	TGGGCATCTGAAGCCTTTTG	GATCTGGTCACCCACGATGAA
Gstt1	CTTGCTCTACCTGGCACACA	CTTCTCCGAAGGCCCGTATG
Gstt2	GTACCAGGTGGCAGACCACT	GTTGCAGAACCAGGACCATT
Gstt3	TCCAGCTGCGTACCATAGAG	ACACTCTCTGCCAAGACGAA
Nqo1	TATCCTTCCGAGTCATCTCTAGCA	TCTGCAGCTTCCAGCTTCTTG
Papss2	ACCTTGGAGACCGAAGGTTT	TTCTTGGCAACAATGAACCA
Por	GGCAAGGAGCTGTACCTGAG	CGACGAGGCAATGGAATAGT
Sult1a1	GGATGTAGCTGAGGCAGAGG	CAGCTCCCAGTGGCATTTAT
Sult1b1	GGTGGGAAAAGAGGGAAGAG	AAGGCCTCTTCATCCAAGGT
Sult1d1	GCCGTCTCCTCGAATAGTGA	TTCCCACCAGCTCTTCACAT
Sult1e1	TCCGTATGGTTCCTGGTATGA	GTTGAACGATTCTGTCCACAAG
Sult2a1	ATTTGGAACCGCTCACCCTGGATA	GCCTGGGCCTTGGAACTGAAGAAA
Sult2b1	AAGGCATTCTTCAGCTCCAA	GAAGGAACTGGTCGGGTGTA
Sult3a1	GGACCTCAGAAGCTCAGTGC	TTTGCTCTTGGGTCAGCTTT
Sult5a1	CCAGTCCAAGATGGGTGACT	AGACCAGGGTTGTAGCATGG
Ugt1a1	CACCTGAAGCCTCAATACCAT	CAGTCCGTCCAAGTTCCACC
Ugt1a5	ACACCGGAACTAGACCATCG	ATACCATGGGAGCCAGAGTG
Ugt1a6	ATACCATGGGAGCCAGAGTG	ACCAGAACTGTGAGGGTTGG
Ugt1a7	TCTCAACCTGCCCTCTGTCT	GTGGGCTGAGAATTTGGTGT
Ugt1a9	CTGGTTCAGCCAGAGGTTTC	TTGGCGACAATTAATCCACA
Ugt2a3	CCCAGAAGGTTTTGTGGAGA	CCACCATGTGTGATGAAAGC
Ugt2b1	CTACAAGTGGATCCCCCAGA	AGGAATGCCATGGTAGATCG
Ugt2b34	AGCTGCCAAAGCAGTCATTT	GCCAGGATCACATCAAACCT
Ugt2b35	GCTCAACTGCTCCAGATTCC	GGCCACCTAATCCTGACAAA
Ugt2b36	TGTGGGAAGGTGTTGGTATGG	TCCACAGCCTTTGCAAAAATAA
Ugt2b36/37/38	GTGGGGCCAACAGTGTCTAT	GTAACAGCTGCTCCTTTGGC
Ugt2b5	ATGTTGGAGGACTCCATTGC	TTGCGTTGGCTTTTTCTTCT

Table s3. ChIP-qPCR primers, targeted genomic regions and motifs.

Targeted genomic regions	qPCR primer sequences	Antibody used	Motifs
Site 1. Cyp3a11, upstream	Forward: CCAGGGATCAAGCCAGTAGATG Reverse: CACAGAATGTTAGCTCAAAGTA	PXR	DR-3 DR-4
Site 2. Cyp3a11, upstream	Forward: CATCTACCCTGCAATGTTGTGAG Reverse: TAGAACAACATGGTCTCTTGGAT	PXR	DR-3
Site 3. Cyp3a25, upstream	Forward: GCCACTTGCACAATGCTCG Reverse: TAGTGCCAATAGATGGATTTGAGC	PXR	ER-6
Site 4. Cyp3a25, upstream	Forward: TGGCCCGGGTTAAACATCAA Reverse: TCAGACCACATGTCTACCCCT	PXR	DR-3
Site 5, Cyp3a59	Forward: AGCGTTGGTGTTGTCCCTAGTG Reverse: AACAGAGAACTGGACTGACCAC	PXR	DR-4 ER-6
Site 6. Cyp4a10, upstream	Forward: GGGTGACAAATGGGTTCTTGGATA Reverse: AGCAAAGGGCAATGGAATAACT	PPARα	DR-1
Site 7. Cyp4a10, in gene	Forward: TTCTTAGAAAGACATGGGTATGCCA Reverse: TCTGAGAGTCCTGTTGGATGG	PPARα	DR-2
Site 8. Cyp4a31	Forward: CCACGCACTTGCATGTATTCTGA Reverse: TCGAGGTGTGGAAAAGACACAC	PPARα	DR-2
Site 9. Cyp4a31, in gene	Forward: AGTCCACTACCTTATCTTTCCTTCA Reverse: TTATGCTCACCTGATCGCCC	PPARα	DR-1
Site 10. Cyp4a32, upstream	Forward: TGTTCCTTCATTTTAGGGGTGA Reverse: TGCACATTGTACTCTTCTCCTC	PPARα	DR-1
Cyp3a11 promoter	Forward: TCCTCCTCAATGCTTCCCTC Reverse: GGTCAAGTTGGGCTGTGGAT	RNA-Pol-II	TATA box
Cyp3a25 promoter	*Forward: GGGGATGAGCTCCATCTTAGC Reverse: ACACCAGACCTACAAGTTCGAG *Also recognizes Cyp3a57/59 genes	RNA-Pol-II	TATA box
Cyp3a59 promoter	Forward: ACAAATGCCAGGTGGAGAGG *Reverse: TTCAGGCCTCCAAGTTTCCC *Also recognizes *Cyp3a25/57* genes	RNA-Pol-II	TATA box
Cyp4a14 promoter	Forward: TCACTAAATGTTTAGAAACCCGC Reverse: CATTCCCCCTCCCACAAGTAG	RNA-Pol-II	TATA box
Cyp4a32 promoter	Forward: AGCTCTCACAAGTCCAAGACA Reverse: ATCTACTGTTAGTCTACCAAGGC	RNA-Pol-II	TATA box

Supplemental Figure and Table Legends:

Figure s1. The 16S rRNA abundance of universal bacteria, as well as the 8 bacterial components in VSL3, namely *B. breve, B. infantis, B. longum, L. acidophilus, L. bulgaricus, L. plantarum, L. paracasei*, and *S. thermophilus*, in the VSL3 DNA. DNA from VSL3 was extracted as described in MATERIALS AND METHODS, and was loaded in each well of the qPCR reactions at 1ng, 3ng, 10ng, and 30ng. Results are expressed as delta-delta cycle value (calculated as 2^[-(Cq - average reference Cq)] of the quantitative PCR (ddCq) as compared to the universal bacteria.

Figure s2. The mRNA expression of the Cyp4f gene cluster (namely Cyp4f17, 4f16, 4f37, 4f15, 4f14, 4f13, 4f39, and 4f41-ps) in liver samples from CV, CV+VSL3, GF, GF+VSL3, and GF+CV groups. The genomic locations of the Cyp4f genes are displayed using the Integrated Genome Viewer (IGV). RT-qPCR for each gene was performed as described in MATERIALS AND METHODS. Data are expressed as % of the housekeeping gene 18S rRNA. Statistical analysis was performed using ANOVA followed by Duncan's Post Hoc Test with $p<0.05$ considered statistically significant. Treatment-groups that are not statistically different are labeled with the same letter.

Figure s3. The mRNA expression of other phase-I enzymes, namely Cyp2b10, Cyp3a13, Aldh1a7, Aldh4a1, Aldh7a1, Ces2c, and Ces3a, in liver samples from CV, CV+VSL3, GF, GF+VSL3, and GF+CV groups. RT-qPCR for each gene was performed as described in MATERIALS AND METHODS. Data are expressed as % of the housekeeping gene 18S rRNA. Statistical analysis was performed using ANOVA followed by the Duncan's Post Hoc Test with $p<0.05$ considered statistically significant. Treatment-groups that are not statistically different are labeled with the same letter.

Figure s4. The mRNA expression of other phase-I enzymes, namely Fmo1, Fmo2, Fmo4, Akr1b8, Akr1c13, Akr1c19, Akr1d1, Ephx1, and Nqo1, in liver samples from CV, CV+VSL3, GF, GF+VSL3, and GF+CV groups. RT-qPCR for each gene was performed as described in MATERIALS AND METHODS. Data are expressed as % of the housekeeping gene 18S rRNA. Statistical analysis was performed using ANOVA followed by the Duncan's Post Hoc Test with $p<0.05$ considered statistically significant. Treatment-groups that are not statistically different are labeled with the same letter.

Figure s5. The mRNA expression of other phase-II Gst enzymes, namely Gsta1, Gsta3, Gsta4, Gstm4, Gstt1, Gstt2, and Gstt3, in liver samples from CV, CV+VSL3, GF, GF+VSL3, and GF+CV groups. RT-qPCR for each gene was performed as described in MATERIALS AND METHODS. Data are expressed as % of the housekeeping gene 18S rRNA. Statistical analysis was performed using ANOVA followed by the Duncan's Post Hoc Test with $p<0.05$ considered statistically significant. Treatment-groups that are not statistically different are labeled with the same letter.

Figure s6. The mRNA expression of other phase-II Ugt and Sult enzymes, namely Ugt1a1, Ugt1a5, Ugt1a6, Ugt1a7, Ugt2b5, Ugt2b34, Ugt2b35, Ugt2b36, Sult1a1, Sult1b1, Sult1d1, and Papss2 (enzyme that produces the co-substrate for sulfation reactions), in liver samples from CV, CV+VSL3, GF, GF+VSL3, and GF+CV groups. RT-qPCR for each gene was performed as described in MATERIALS AND METHODS. Data are expressed as % of the housekeeping gene 18S rRNA. Statistical analysis was performed using ANOVA followed by the Duncan's Post Hoc Test with $p<0.05$ considered statistically significant. Treatment-groups that are not statistically different are labeled with the same letter.

Figure s7. Genomic locations of positive PXR (A) and PPARα (B) DNA binding sites to the *Cyp3a* (A) and *Cyp4a* (B) gene clusters, respectively. These binding sites were re-analyzed based on previously published ChIP-Seq experiments (Cui et al., 2010; Lee et al., 2014).

Table s1. Primer Sequences and Specificity for the bacterial 16S rRNA quantification.

Table s2: RT-qPCR primer sequences.

Table s3. ChIP-qPCR primers, targeted genomic regions and motifs.